

A Seakeeping Experiment Research On Flokstra Container Ship Model

by

ZHENG-QUAN ZHOU
DE-CAI ZHOU
NAN XIE

(July 20 , 1996)

ABSTRACT

An experiment is carried out to investigate the effect of wave direction and rolling motion on deck wetness and on the relative motion for a large fast container ship. The experiment results of regular waves and irregular waves are presented. From this experiment, it is evident that the wave direction and rolling motion have a considerable influence on relative motion at midship.

1. INTRODUCTION

Technical developments in the ship building and shipping industry, demand reexamination of the " International Convention on Load Lines 1966 " (ICLL 1966) with the aim of developing a tool for the assignment of freeboard which needs to be flexible enough to deal with conventional as well as unconventional ships.

The goal of this research project is to develop freeboard tables conditioned on deck wetness and setting up respective requirements for load line calculations, which will support " International Maritime Organization " (IMO) activities to revise the 1966 convention for a year 2000 release.

According to the requirement of the " SLF Load Lines Working Group ", The Register of Shipping of the People's Republic of China arrange an experiment to investigate the effect of wave direction and rolling motion on deck wetness and on the relative motion for a large fast container ship . China Ship Scientific Research Center undertake this ship model experiment .

This paper is reporting the experiment results and analyzing the phenomena revealed by this experiment.

2. DESCRIPTION OF THE MODEL TEST

2.1 Selection of Wave Directions

The reviews of both experimental and theoretical work on relative motion at present are

largely concerned on head seas. This approach is rational since it has been confirmed that the bow relative motion is largest in head seas when determine the freeboard height at bow . Due to the combined effect of the vertical and lateral motion, however, higher relative motion at midship may occur in oblique waves.

For container ships having a large natural roll period can lead to large motion due to near-synchronous conditions in oblique waves. Therefore, in the present study, measurements of relative motion and deck wetness were carried out at midship and at oblique wave directions.

Summarizing it may be concluded that for a larger container ship the highest relative motion due to vertical 、 lateral motion may be expected in 30 to 60 degree wave directions, either approaching from the bow or from the stern. Within this range no priority can be given to a certain heading. For the present research the model tests were conducted initially in bow and stern quartering waves e.g. approaching 45 degrees off the bow and the stern. Preference was given to 45 degrees heading since in stern quartering waves largest roll angles due to near-synchronous conditions will occur in the wave length and ship speed range tested. It follows that the relative motion was considerably influenced by the roll motion.

2.2 Seakeeping Basin

This ship model experiment is carried out in the seakeeping basin of China Ship Scientific Research Center from June 10 to July 6, 1996.

China Ship Scientific Research Center (CSSRC) is a research and development organization in ship engineering. It offers service in R&D 、 model experimentation and consultation in concept design for various marine structures.

CSSRC's headquarters is located at WuXi, JiangSu province, with a branch office at Shanghai. CSSRC has more than 40 years of history, and has tested and given consultations to most of the large marine structures in China.

Seakeeping basin is one of main facilities in CSSRC. The dimensions of the seakeeping basin are 69m× 46m× 4m (water depth), wave makers on two adjacent sides, capable of generating regular and irregular waves. A bridge spans the diagonal of the basin and is rotatable 45°. Model running or towed by a carriage under the bridge (max. speed 4m/s) may be tested at any required angle with respect to the waves. Wind and current effect also may be simulated.

2.3 Ship Model

The tested ship is a container ship provided by “ SLF Load Lines Working Group ” referred to as the “ Flokstra-Ship ”. The main particulars of the ship are listed in Table 1 and a body plan is reproduced in Figure 1 as well as the stem and stern outlines in Fig.2, two ship model photo in Fig. 3 and Fig. 4.

The ship model has an integral hull form including the hull form above waterline, an integral deck form, as well as a set of appendages: bilge keels, propeller shafts, shell bossing, two propellers, a rudder.

The ship model constructed to a scale of 1 to 80 of glass reinforced polyester .

The scale was mainly determined by the capacity of the irregular wave generator installed in the Seakeeping Laboratory of the CSSRC .

The model was fitted with bilge keels .

Table 1 Principal Ship Dimensions

No.	Denomination	Symbol	Full Scale	Ship Model
1	Total length	L_{OA}	284.0m	3.55m
2	Length between perpendiculars	L_{PP}	270.0m	3.375m
3	Breadth	B_{WL}	32.2m	402.5mm
4	Total height	H	18.662m	233.3mm
5	Displacement volume	∇	56097m ³	0.1096m ³
6	Displacement weight	Δ	57499t.	109.6kg
7	Draught even keel	T	10.85m	135.6mm
8	Block coefficient	C_B	0.598	0.598
9	Center of gravity above base	Z_g	13.49m	168.6mm
10	L.C.G. aft of station 10	X_g	-10.12m	-125.6mm
11	Transverse gyradius in roll direction	K_{XX}	0.375 B_{WL}	0.375 B_{WL}
12	Longitudinal gyradius in pitch direction	K_{yy}	0.248 L_{WL}	0.248 L_{WL}
13	Metacentric height	GM	1.15m	14.4mm
14	Natural roll period	T_ϕ	24.9s	2.78s
15	Natural pitch period	T_θ	8.6s	0.96s
16	Length of bilge keel	l	47.0m	587.5mm
17	Breadth of bilge keel	b	0.48m	6.0mm
18	Diameter of propeller	d	6.56m	82.0mm

2.4 Model Preparation And Calibration

The weight distribution in the model was adjusted on a low — mass trimming table , by means of which the exact position of the center of gravity in the vertical and horizontal directions was obtained .

The longitudinal radius of gyration in pitch direction was adjusted on the trimming table, whereas the transverse radius of the gyration in roll direction was adjusted and verified by a roll heeling experiment in still water.

2.5 Test Content

The primary aim of the present experiment is to investigate the effect of wave direction , wave height , period and ship speed, as well as rolling motion on relative motion and deck wetness at midship.

The main test contents are rolling decay test, regular wave test and irregular wave test.

The main measurements in this ship model experiment are :

- a) Determining the roll damping in still water ;
- b) Measuring the heave , pitch and roll motion of ship model in regular and irregular

waves ;

- c) Measuring the relative motion in several stations ;
- d) Measuring the frequencies of deck wetness in several stations ;
- e) Measuring the vertical acceleration at bow part of the ship .

2.6 Test Procedures

During the tests the model was self — propelled by two stock propellers . The model was completely free in its motions . It was kept on course by an auto — pilot , controlling the rudder in such a way that a straight course through the middle of the basin was maintained by small rudder angles . The model was connected by a light — weight vertical rod in the center of gravity of the model to a low — mass and low — friction subcarriage , So that no appreciable forces or moments were transmitted on the model .

Each test run contained simultaneous recordings of the following quantities by data recording computers .

— Heave , pitch and roll angles , recorded by a six — degree freedom motion measuring system connected to the light — weight rod .

— Relative motion (with respect to the wave surface) at the bow and the stern as well as at amidship , obtained by resistance wire wave probes attached vertically on the model at the station of 17 , 14 , 10 and 5 on the weather-side .

— Vertical acceleration at the station 17 , measured by a 2g accelerometer .

— Model speed , measured by a slotted disc with photo cell pick-up .

Wave height , determined by two wave probes , one fixed to the moving carriage in front of the ship model, another fixed on the center at basin . The wave probes were calibrated before the tests.

In irregular wave case , the frequency and probability of deck wetness at station 17 , 14 , 10 and 5 , recorded by a computer .

The requirement of velocity simulated in model test is listed in Table 2 .

Table 2 Velocity Simulated of Ship Model

No.	Full scale (knot)	Ship model (m/s)	Fn
1	0	0	0
2	10	0.575	0.10
3	22	1.265	0.22
4	27	1.553	0.27

3. ANALYSIS OF TEST RESULTS IN ROLL DAMPING TEST

Roll damping tests were first performed in calm water at a speed of 0.0, 10.0, 22.0 and 27.0 knots to determine the roll damping coefficients. During test, a transient moment acting on the ship model, then, recording the curve of declining roll angle history. Analysis the declining curve, measuring the period of roll motion and the roll damping coefficients.

The test content is listed in Table 3.

Table 3 The Content of Roll Damping Test

No.	Ship model velocity (m/s)	Full scale speed (knot)	Test content
A-01	0	0	The history of rolling angle
A-02	0.575	10	
A-03	1.265	22	
A-04	1.553	27	

3.1 Natural Period of Roll

According to the measured declining curve, the period of roll for every time can be found. Averaging several periods, finding the curve of rolling period to Froude number as Fig.5. In Fig.5, there is a little variation of rolling period as the increase of velocity. The exact results of rolling period list in Table 4.

Table 4 Results of Natural Period of Rolling Motion

F _n	0	0.10	0.22	0.27
T _φ (s)	24.6	24.8	23.7	23.8

3.2 Roll Damping Coefficient

A curve of relative declining roll angle can be obtained according to the roll damping test. Fig. 6 is the relative declining angle curve at the zero forward speed condition. In Fig.6, $\Delta\phi$ is the declining value of rolling angle in every half period, ϕ is the average roll angle. The rolling damping moment can be formulated as following relation in linear condition.

$$M(\dot{\phi}) = B_1 \dot{\phi} \quad (2)$$

in which

$$B_1 = \frac{2 Dh}{\pi n_\phi} a \quad (3)$$

Where "a" is average value of relative declining angle in Fig.6, D the displacement volume, h metacentric height. In the free rolling case, $n_\phi = \omega_e$, the non-dimensional roll damping coefficient represents as :

$$2\mu_\phi = \frac{2 \Delta\phi}{\pi \phi} = \frac{2a}{\pi} \quad (4)$$

Linearizing, finding the value a and the non-dimensional roll damping coefficients as Table 5. Roll damping coefficients $2\mu_\phi$ varies according to the average roll angle shown in fig.7.

Table 5 Non-dimensional Roll Damping Coefficients

F_n	0	0.1	0.22
a	0.1519	0.2461	0.6261
$2\mu_\phi$	0.0968	0.1566	0.3985

The variation of $2\mu_\phi$ according to the ship velocity, shown in Fig.8. For FLOKSTRA container ship, roll damping coefficient has little change as the increasing of roll angle ; however, there is large change as the increasing of velocity.

4. DISCUSSION OF REGULAR WAVE TEST RESULTS

4.1 Content of Regular Wave Test

The regular wave tests were conducted with different wave directions , since the roll motion has an importance influence on determining the freeboard height at midship. The wave angles are head sea , beam sea and oblique wave(135°).

The speeds are 10 and 22 knots .

At each headings , tests were conducted in 15 regular waves with lengths varying between a ratio of $\lambda/L=0.4 \sim 3.5$; the wave height was kept constant at 70.0 mm .

The results of the regular wave tests will ultimately be used to check the theoretical computer program, therefore the accuracy of the test result must be required. On the another hand, the results of the regular wave test will be used to predict the response in irregular seas by the linear superposition principle, therefore the selected wave frequency range in regular wave tests covers the main part of wave energy in irregular seas and is sufficiently large to minimize the inaccuracy in the prediction due to the extrapolation of the ship responses.

All measuring signals were recorded on hard disk of a computer after magnified by a signal magnifier.

The content of experiment is listed in Table 6.

Table 6 Test Content and Headings in Regular Wave

Test No.	wave direction	Ship model velocity (m/s)	Test content
B—01	180°	0.575	Wave , roll , pitch , heave , the relative motion at station 17 [#] 、 14 [#] 、 10 [#] 、 5 [#] and vertical acceleration at station 17 [#]
B—02	180°	1.265	
B—03	135°	0.575	
B—04	135°	1.265	
B—05	90°	0.575	
B—06	90°	1.265	

4.2 Analysis of Regular Wave Test Results

Harmonic analysis was applied to determine the first harmonic of the measured signals having the encounter frequency of the waves. This analysis is necessary in view of the higher frequency oscillations which were superimposed upon the recording traces. Then time analysis is applied to determine the amplitude, mean value by averaging the recordings over a number of cycles.

The measured motion responses are presented as amplitude transfer functions versus wave length/ship length ratio. The figures of results are listed as Table 7. In those figures, all parameters are dimensionless, the meanings of parameters see symbols set, "Δ." is the results of tests, lines represented as the theoretical results by the strip theory. Other condition also listed in those figures.

**Table 7 The Frequency Response Function Curves
in Regular Wave Test**

Test No.	B-01	B-02	B-03	B-04	B-05	B-06
Wave direction (deg.)	180	180	135	135	90	90
Full scale speed (knot)	10	22	10	22	10	22
Pitch	Fig.9	Fig.10	Fig.11	Fig.12	/	/
Roll	/	/	Fig.13	Fig.14	Fig.15	Fig.16
Heave	Fig.17	Fig.18	Fig.19	Fig.20	Fig.21	Fig.22
Relative motion at station 17	Fig.23	Fig.24	Fig.25	Fig.26	Fig.27	Fig.28
Relative motion at station 14	Fig.29	Fig.30	Fig.31	Fig.32	Fig.33	Fig.34
Relative motion at station 10	Fig.35	Fig.36	Fig.37	Fig.38	Fig.39	Fig.40
Relative motion at station 5	Fig.41	Fig.42	Fig.43	Fig.44	Fig.45	Fig.46
Vertical acceleration at station 17	Fig.47	Fig.48	Fig.49	Fig.50	Fig.51	Fig.52

4.2.1 Pitch Response

Fig. 9 ~ Fig. 12 are the pitch responses. In those figures, The pitch response in head seas were much larger than in bow waves (135°) ; the pitch response is increasing as the increasing of velocity.

4.2.2 Roll Response

Fig. 13 ~ Fig. 16 are the roll responses. In those figures, The roll response in beam waves were much larger than in bow waves (135°) ; as the increasing of velocity, the roll response is decreasing because of the roll damping sharply increasing.

4.2.3 Heave Response

Fig. 17 ~ Fig. 22 are the heave responses. In the case of beam waves, the heave response ratio tends to 1.0 since the heave motion response is essentially synchronous with waves ; The heave response in bow oblique waves(135°) is larger than in head waves ; the heave response is decreasing as the increasing of velocity.

4.2.4 Relative Motion At Station 17

The transfer function of relative motion at station 17 are shown in Fig.23~28. From those figures, one can see that the response in bow quarter(135°) wave are larger than in head wave and beam waves; the relative motion in head waves are large than that of in beam waves. the larger the speed, the higher the relative motion amplitude.

4.2.5 Relative Motion At Station 14

Fig 29~34 show the transfer functions of relative motion at station 14, the tendency is similar to that of station 17.

4.2.6 Relative Motion At Station 10

Fig.35~40 show the transfer functions of relative motion at station 10 (midship). The relative motion amplitude in beam waves are little larger than that in bow oblique wave and head waves. The relative motion in bow oblique waves are larger than that of in head waves.

4.2.7 Relative Motion At Station 5

Fig.41~46 show the transfer function of relative motion at station 5. The relative motion amplitude in beam waves , bow oblique wave and head waves are almost the same. The relative motion in bow oblique waves are little larger that those in head waves and in beam waves.

4.2.8 Vertical Acceleration At Station 17

Fig.47~52 show the transfer functions of vertical acceleration at bow. The acceleration in bow oblique waves and head waves are larger than that in beam waves . The larger the ship speed, the larger the vertical acceleration.

In general, the larger the ship speed, the larger the response of pitch, heave, relative motion and vertical acceleration, the smaller the roll response. The relative motion transfer functions in bow oblique wave are larger than that in head waves. The test results are in good agreement with the theoretical predictions.

5 TESTS IN IRREGULAR WAVES

5.1 Test Contents

The tests are carried out by using self-propelled model in irregular waves, and the test runs are listed in Table 8. For each test run, roll 、 heave 、 pitch 、 vertical acceleration at bow 、 relative motion at stations 17, 14, 10 and 5 are measured, and the number of deck wetness in each run are obtained. Wave headings are head sea, bow quarter and beam seas.

According to the specification of seakeeping model tests, the test period are corresponding to one

hour at full scale time. During the test, both the wave at a fixed point in the basin and the encounter wave at the front of the ship model are measured by wave probes.

Table 8 Test Content and Headings in Irregular Wave

Test No.	Wave direction (deg.)	Full scale speed (knot)	Significant wave height (m)	Average wave period T_{01} (s)	Test Content
C-01	180	22	8.37	14.10	Wave, roll, pitch heave, the relative motion at station 17 [#] , 14 [#] , 10 [#] , 5 [#] , deck wetness and vertical acceleration at station 17 [#]
C-02		10	7.15	12.88	
C-03	135	10	8.25	12.25	
C-04		10	7.19	11.99	
C-07		22	7.72	12.25	
C-05	45	10	7.67	11.00	
C-06		22	8.68	11.20	

5.2 Results of Irregular Wave Test

Basing on the curves of calibration, the voltages are changed into physical signals after A/D. These signals are analyzed by using spectral technical, and yielding significant values of each responses.[3]

The statistical values in irregular tests are listed in Tables 9 and 10, these values are corresponding to the full scale ship, and the responses are significant single amplitudes, roll and pitch are in degree.

Table 9 The Statistical Values in Irregular Wave Tests

No.	Test No.		C-01	C-02	C-05	C-06
	Wave direction (deg.)		180	180	45	45
	Full scale speed (knot)		22	10	10	22
1	Wave	$S_{1/3}$ (m)	8.37	7.15	7.67	8.68
		T_{01e} (s)	9.30	10.02	15.38	22.36
2	Relative motion at station 17	$S_{1/3}$ (m)	6.99	5.16	3.34	7.80
3	Relative motion at station 14	$S_{1/3}$ (m)	3.36	1.55	3.10	3.55
4	Relative motion at station 10	$S_{1/3}$ (m)	2.15	2.36	5.23	6.39
5	Relative motion at station 5	$S_{1/3}$ (m)	2.48	2.16	2.99	7.33
6	Roll	$\phi_{1/3}$ (deg.)	/	/	5.34	17.61
7	Pitch	$\theta_{1/3}$ (deg.)	2.60	2.19	1.61	1.76
8	Heave	$Z_{1/3}$ (m)	3.06	1.70	1.80	1.98
9	Vertical acceleration at station 17	$A_{1/3}$ (g)	0.301	0.146	0.065	0.069

Table 10 The Statistical Values in Irregular Wave Tests

No.	Test No.		C-03	C-04	C-07
	Wave direction (deg.)		135	135	135
	Full scale speed (knot)		10	10	22
1	Wave	$S_{1/3}$ (m)	8.25	7.19	7.72
		T_{01c} (s)	10.11	9.84	8.32
2	Relative motion at station 17	$S_{1/3}$ (m)	6.25	5.62	7.50
3	Relative motion at station 14	$S_{1/3}$ (m)	2.92	2.64	4.13
4	Relative motion at station 10	$S_{1/3}$ (m)	3.04	2.71	2.45
5	Relative motion at station 5	$S_{1/3}$ (m)	3.82	3.44	3.12
6	Roll	$\phi_{1/3}$ (deg.)	8.62	6.34	3.69
7	Pitch	$\theta_{1/3}$ (deg.)	2.56	2.11	2.57
8	Heave	$Z_{1/3}$ (m)	2.28	2.24	3.10
9	Vertical acceleration at station 17	$A_{1/3}$ (g)	0.236	0.200	0.384

For the test conditions, numerical predictions are given by a strip theory program and compared with the model test. These are shown in Table 11-A~Table 11-D.

Table 11-A Calculated And Measured Tests Statistical Values in Irregular Wave

Full scale speed (knot)	22		10	
Wave direction (deg.)	180		180	
Sea state	$H_{1/3}=8.37m$ $T_{01}=14.10s$		$H_{1/3}=7.15m$ $T_{01}=12.88s$	
Test No.	C-01		C-02	
	Calculatio n	Experimen t	Calculatio n	Experimen t
Relative motion at station 17 (m)	6.35	6.99	4.43	5.16
Relative motion at station 14 (m)	3.50	3.36	1.92	1.55
Relative motion at station 10 (m)	1.74	2.15	2.18	2.36
Relative motion at station 5 (m)	2.26	2.48	2.32	2.16
Roll (deg.)	/	/	/	/
Pitch (deg.)	2.77	2.60	2.17	2.19
Heave (m)	3.04	3.06	1.94	1.70
Vertical acceleration at station 17 (g)	0.268	0.301	0.137	0.146

**Table 11-B Calculated And Measured The Statistical Values
in Irregular Wave**

Full scale speed (knot)	10		10	
Wave direction (deg.)	135		135	
Sea state	$H_{1/3}=8.25\text{m}$ $T_{01}=12.25\text{s}$		$H_{1/3}=7.19\text{m}$ $T_{01}=11.99\text{s}$	
Test No.	C-03		C-04	
	Calculatio n	Experimen t	Calculatio n	Experimen t
Relative motion at station 17 (m)	5.24	6.25	4.72	5.62
Relative motion at station 14 (m)	2.95	2.92	2.67	2.64
Relative motion at station 10 (m)	2.17	3.04	1.94	2.71
Relative motion at station 5 (m)	2.90	3.82	2.62	3.44
Roll (deg.)	/	8.62	/	6.34
Pitch (deg.)	2.55	2.56	2.23	2.11
Heave (m)	2.65	2.28	2.23	2.24
Vertical acceleration at station 17 (g)	0.200	0.236	0.179	0.200

**Table 11-C Calculated And Measured The Statistical Values
in Irregular Wave**

Full scale speed (knot)	22			
Wave direction (deg.)	135			
Sea state	$H_{1/3}=7.72\text{m}$ $T_{01}=12.25\text{s}$			
Test No.	C-07			
	Calculatio n	Experimen t	Calculatio n	Experimen t
Relative motion at station 17 (m)	6.35	7.50		
Relative motion at station 14 (m)	4.14	4.13		
Relative motion at station 10 (m)	2.27	2.45		
Relative motion at station 5 (m)	2.61	3.12		
Roll (deg.)	/	3.69		
Pitch (deg.)	2.58	2.57		
Heave (m)	2.97	3.10		
Vertical acceleration at station 17 (g)	0.299	0.384		

**Table 11-D Calculated And Measured The Statistical Values
in Irregular Wave**

Full scale speed (knot)	10		22	
Wave direction (deg.)	45		45	
Sea state	$H_{1/3}=7.67m$ $T_{01}=11.00s$		$H_{1/3}=8.68m$ $T_{01}=11.20s$	
Test No.	C-05		C-06	
	Calculatio n	Experimen t	Calculatio n	Experimen t
Relative motion at station 17 (m)	3.35	3.34	4.24	7.80
Relative motion at station 14 (m)	2.27	3.10	2.97	3.55
Relative motion at station 10 (m)	2.70	5.23	3.64	6.39
Relative motion at station 5 (m)	2.56	2.99	2.37	7.33
Roll (deg.)	/	5.34	/	17.61
Pitch (deg.)	1.68	1.61	1.74	1.76
Heave (m)	1.80	1.80	2.00	1.98
Vertical acceleration at station 17 (g)	0.057	0.065	0.033	0.069

5.2.1 Effect of Wave Heading

Relative motion at each station varying with heading angles is listed in Table 12. For the statistical values of relative motion at stations 14, 10 and 5, significant values in bow quarter and quarter following waves are larger than those of in head waves. In quarter following waves largest roll angles may occur due to roll resonance, relative motions are even larger than in head waves.

**Table 12A The Significant Value of Relative Motion /Significant Wave Height
($S_{1/3}/H_{1/3}$)**

Speed $V_s=10knot$

Angle	45°	135°	180°
Station			
17 [#]	0.436	0.782	0.722
14 [#]	0.404	0.367	0.217
10 [#]	0.682	0.377	0.330
5 [#]	0.390	0.478	0.302

Table 12B The Significant Value of Relative Motion /Significant Wave Height
 $(S_{1/3}/H_{1/3})$

Speed $V_s=22$ knot

Angle Station	45°	135°	180°
17 [#]	0.897	0.972	0.835
14 [#]	0.409	0.535	0.401
10 [#]	0.736	0.313	0.257
5 [#]	0.845	0.404	0.296

5.2.2 Effect of Ship Rolling

In order to demonstrate the effect of rolling to relative motion, the test results of relative motion at station 10 are listed in Table 13.

Form Table 13, it is seen that, in test run No. C-06, the encounter wave period are approximate to the roll natural period, the ship is in roll resonance condition, large roll motion is excited, therefore, relative motion is also large. Thus, when determining the freeboard at midship, the effect of rolling on relative motion can not be neglected.

Table 13 Effect of Ship Rolling

Test No.	C-01	C-02	C-03	C-04	C-07	C-05	C-06
Wave direction (deg.)	180		135			45	
Full scale speed (knot)	22	10	10	10	22	10	22
Encounter wave period T_{01e} (s)	9.30	10.02	10.11	9.84	8.32	15.38	22.36
Natural roll period (s)	/	/	24.80	24.80	23.70	24.80	23.70
Roll (deg.)	/	/	8.62	6.34	3.69	5.34	17.61
The relative motion at station 10/significant wave height	0.257	0.330	0.368	0.377	0.317	0.682	0.736

5.2.3 Coefficient of Dynamic Swell up

The dynamic swell up coefficient is defined as:

$$SUC = \frac{S}{S_0} \quad (5)$$

where S is the real relative vertical motion, S_0 is the notional relative motion which defined by absolute motion minus incident wave surface elevation. The measured dynamic swell-up coefficients are listed in Table 14. the dynamic swell up coefficients at bow are between 1.1~1.2.

Table 14. Coefficient of Dynamic Swell up

Test No.	C-02	C-03	C-04	C-05	C-01	C-07
Coefficient of dynamic swell up	1.16	1.19	1.19	1.00	1.10	1.18
Average	1.14					

6. CONCLUSION

From present seakeeping model experiment, test results of motions and relative motions for the Flokstra ship in regular and irregular waves, at head sea, bow quarter, beam sea, quarter following directions are obtained, which will be used to check on the computer program. It can be concluded that the wave direction and rolling motion have a considerable influence on relative motion at midship. Thus, when determining the freeboard at midship based on the deck wetness, only the effect of head wave taken into account is not sufficient, the effect of oblique waves should also be taken into account.

REFERENCES

- [1] Zhou.Z.Q, Xie. N and Gu M et al.: " Seakeeping Model Test Program for the Flokstra Ship " , CSSRC Technical Report, March,1996.
- [2] Peng.Y.S: "Seakeeping", China Defense Press,1989.
- [3] Xie. N, Zhou. Y.N et al.: " Data Processing of Seakeeping and Ocean Engineering Model Tests " , CSSRC Technical Report,Dec,1991.

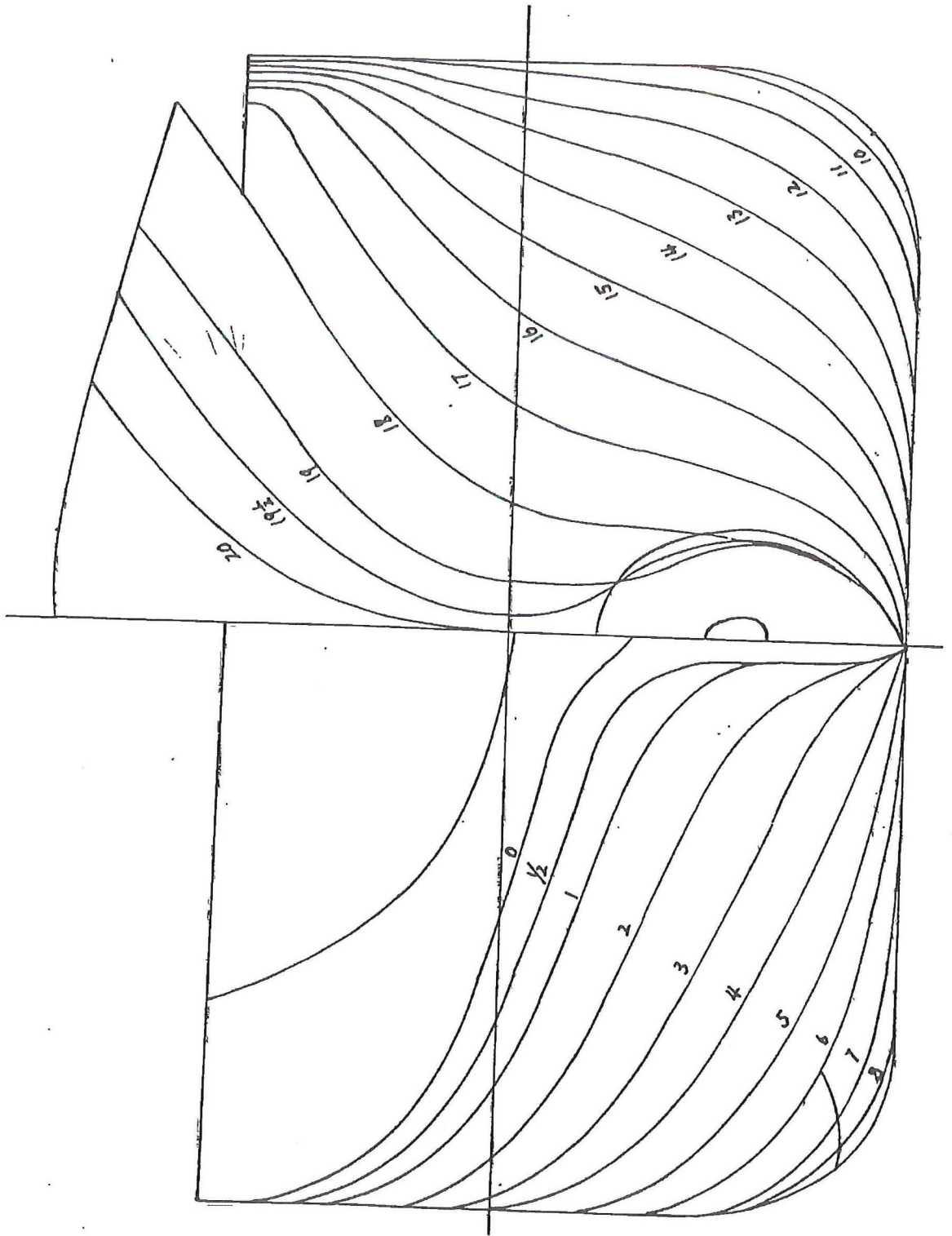


Fig.1 Body Plan

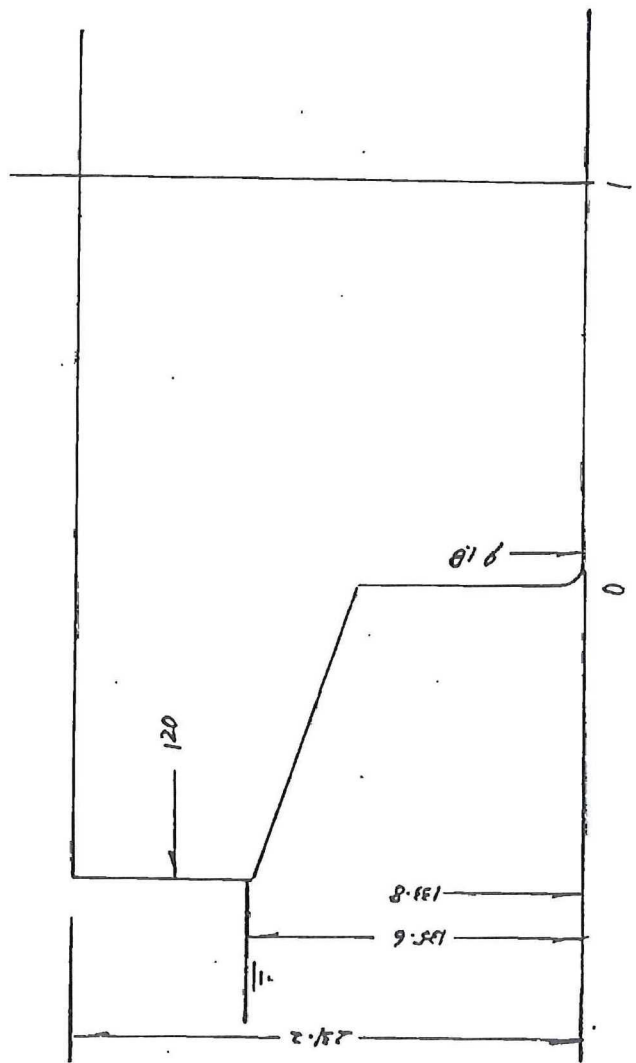
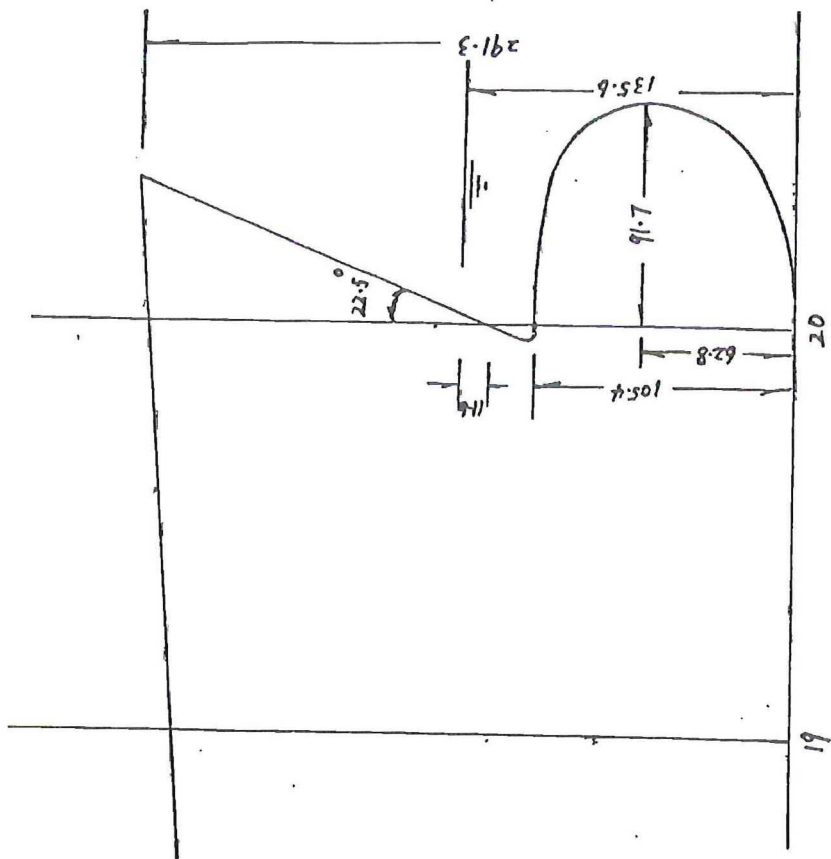


Fig.2 The Stem And Stern Outlines (Unit:mm)

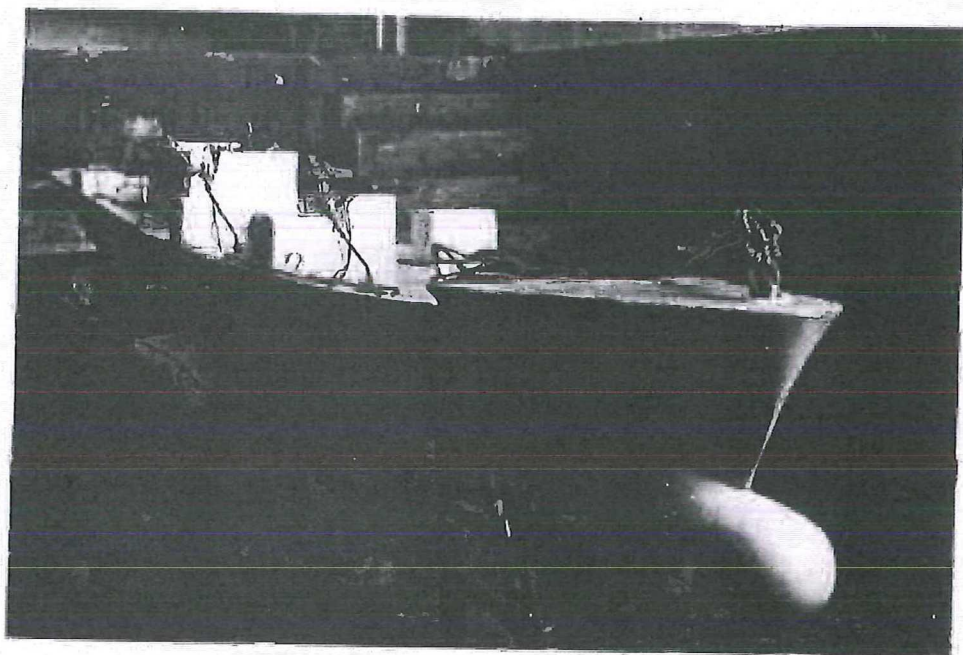


Fig.3 Model Test Preparation

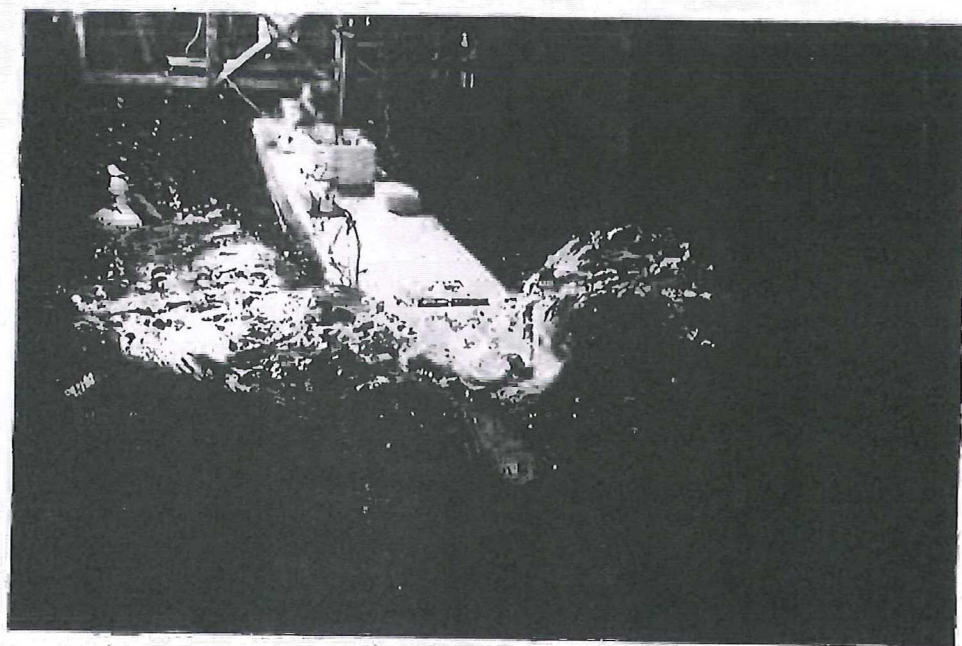


Fig.4 Model Test In Irregular Wave

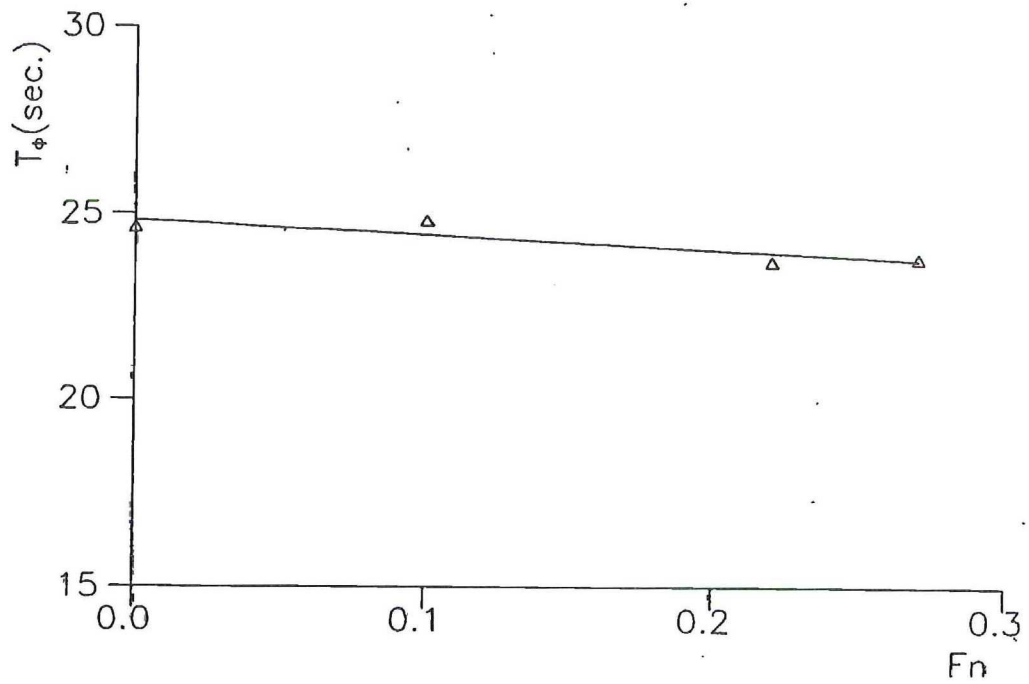


Fig.5 Natural period of roll

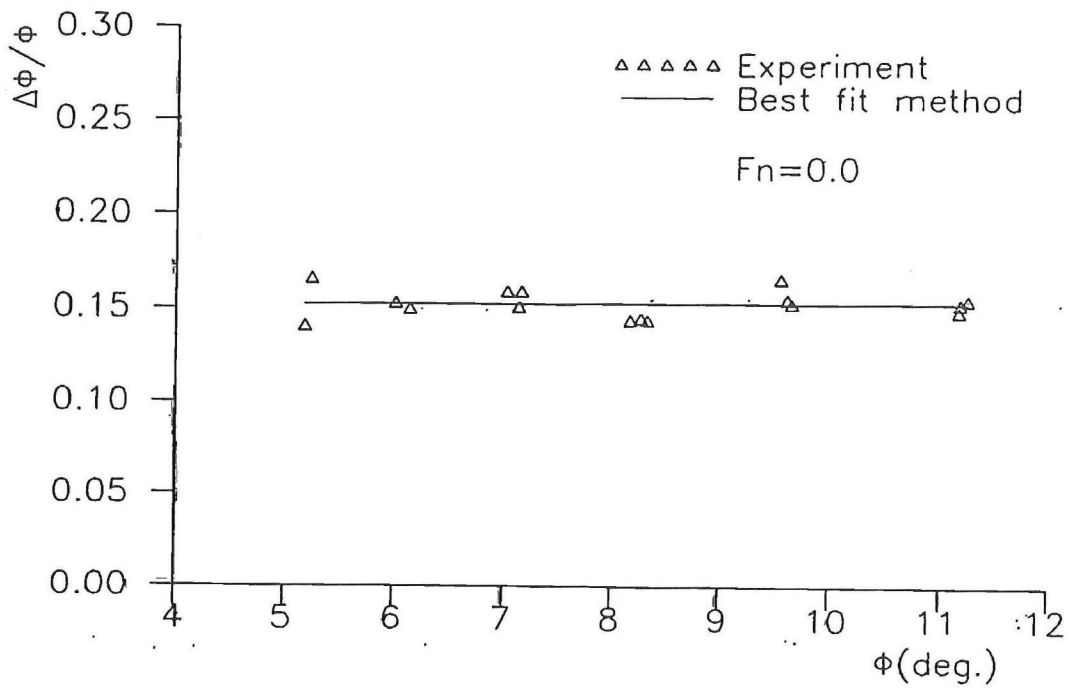


Fig.6 Relative decay amplitude

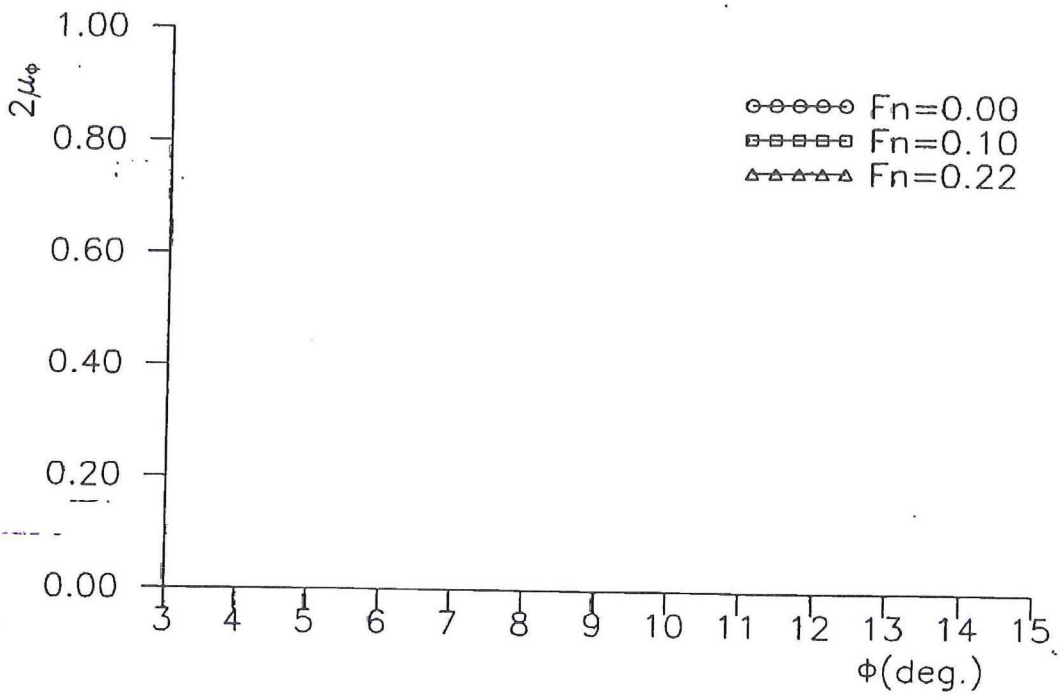


Fig.7 Roll damping coefficient

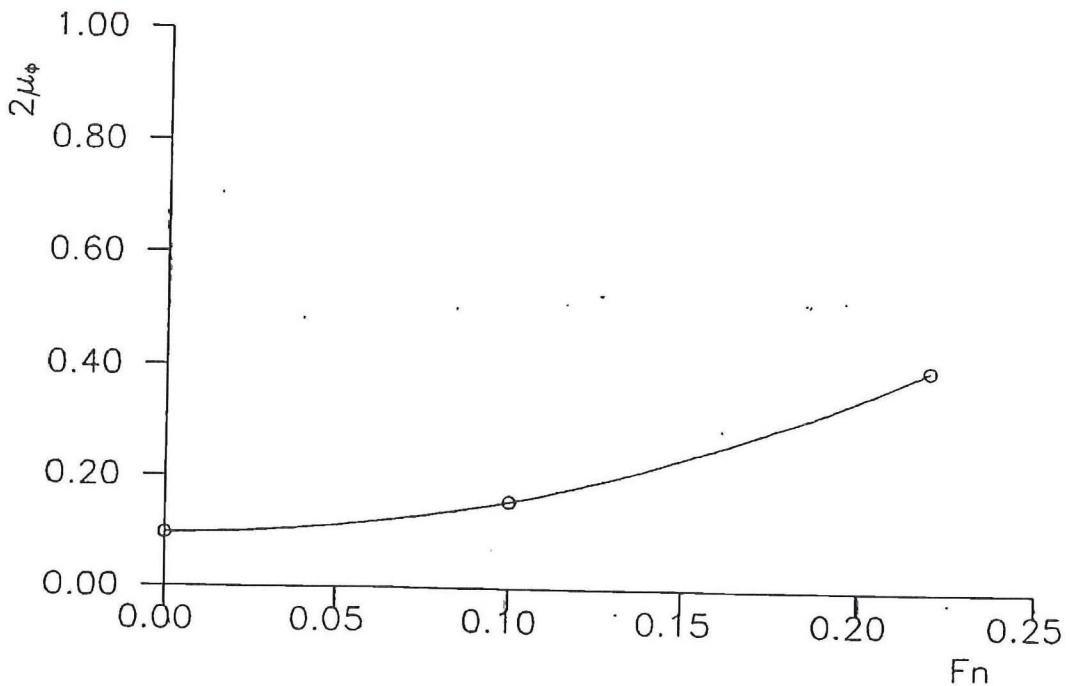


Fig.8 Roll damping coefficient

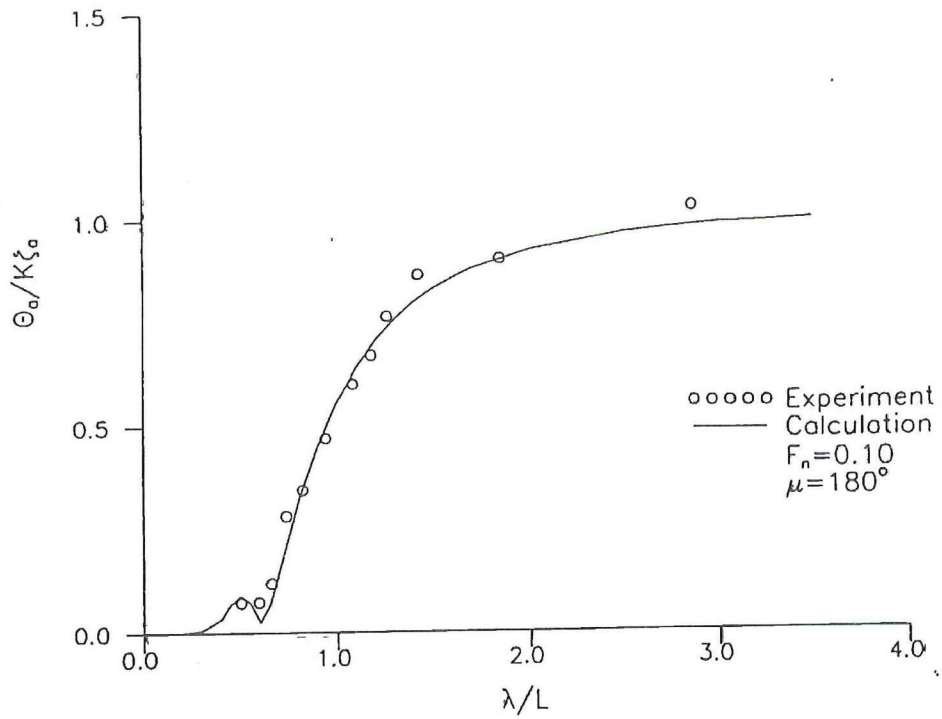


Fig.9 Calculated and measured pitch transfer function

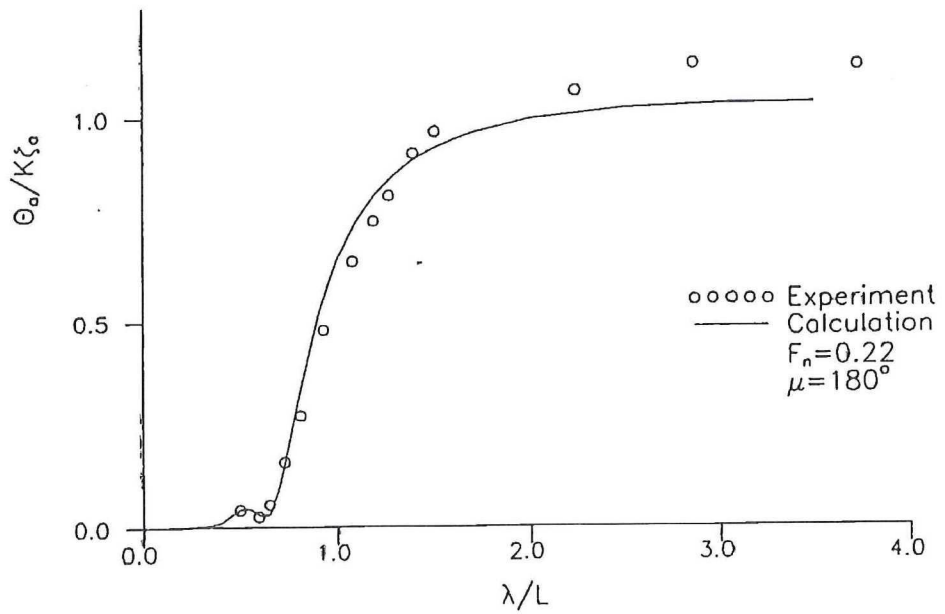


Fig.10 Calculated and measured pitch transfer function

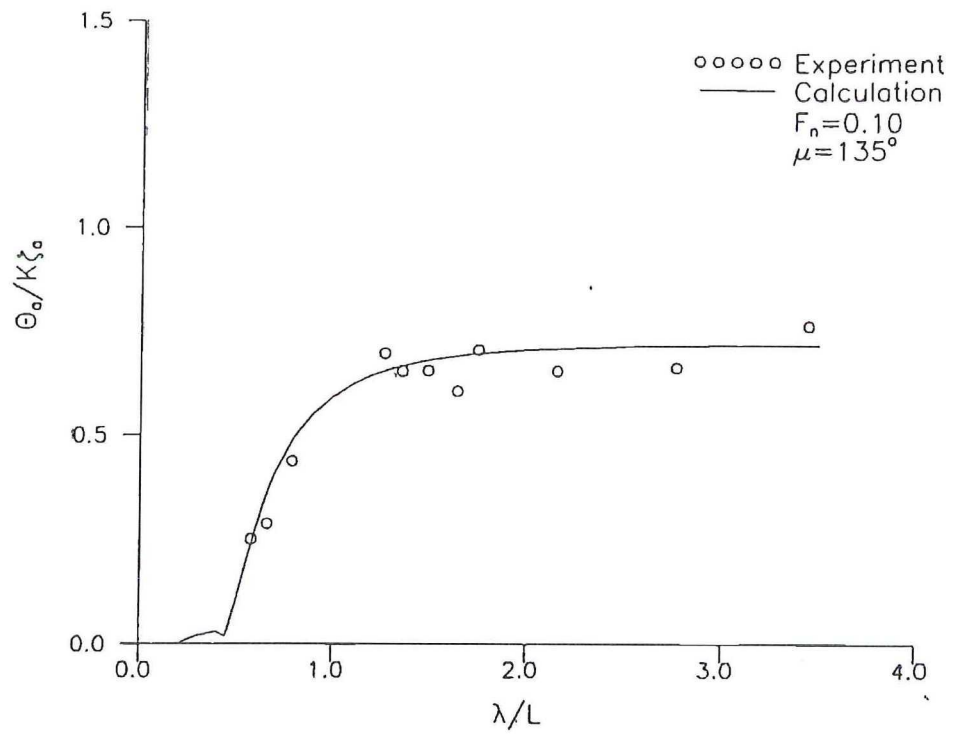


Fig.11 Calculated and measured pitch transfer function

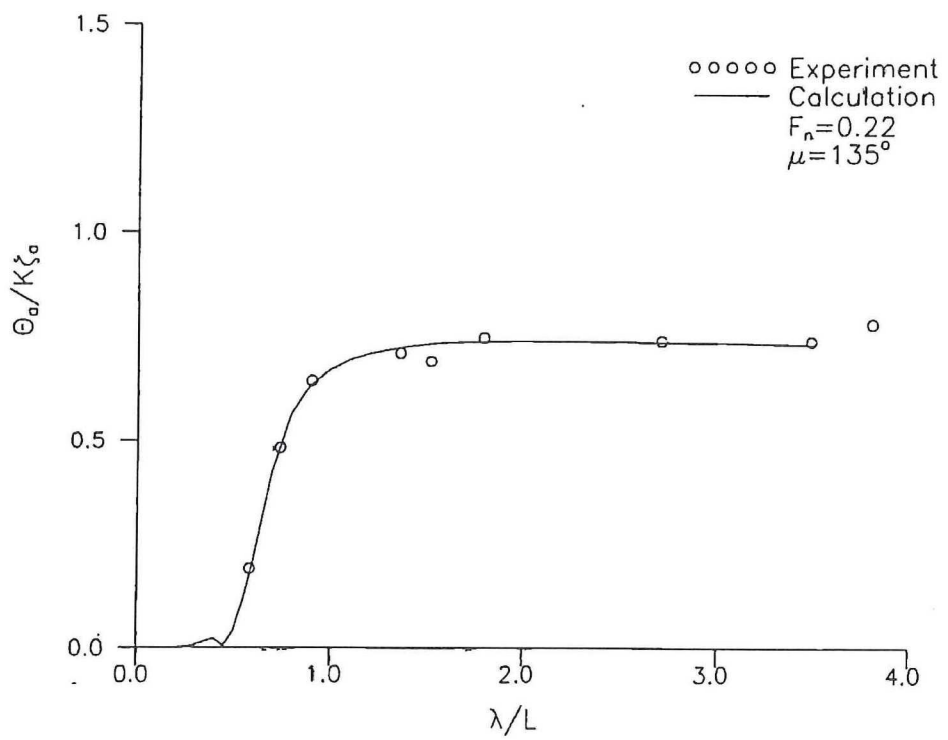


Fig.12 Calculated and measured pitch transfer function

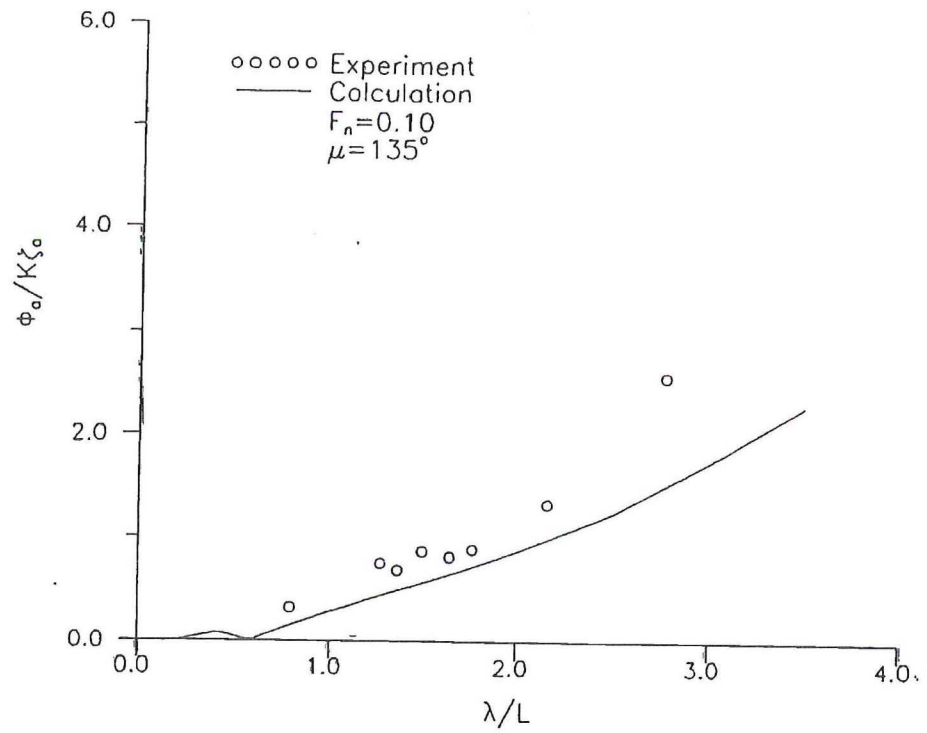


Fig.13 Calculated and measured roll transfer function

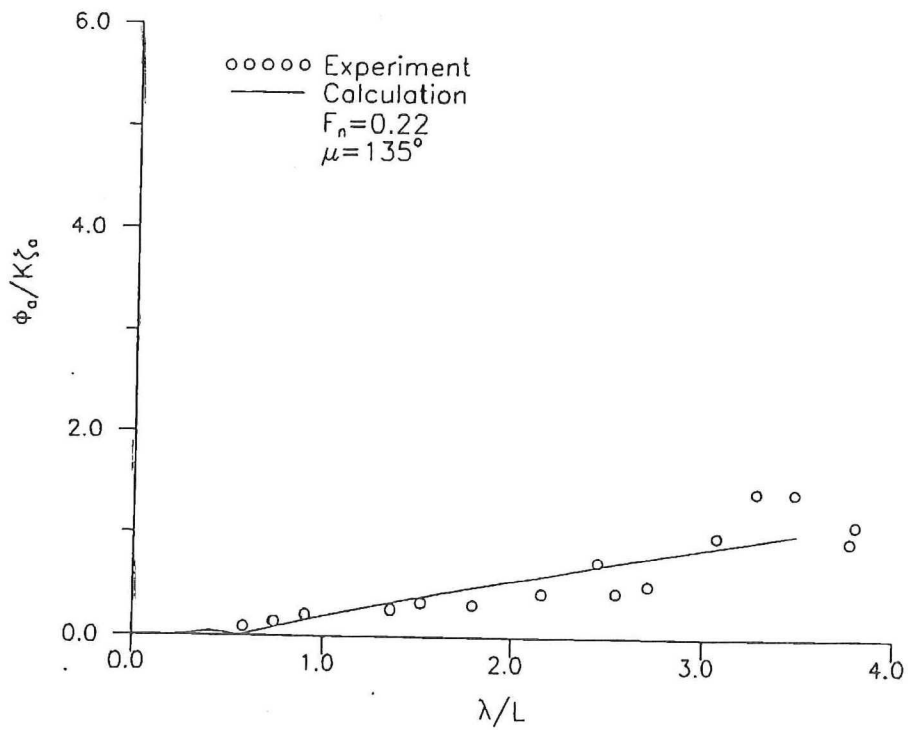


Fig.14 Calculated and measured roll transfer function

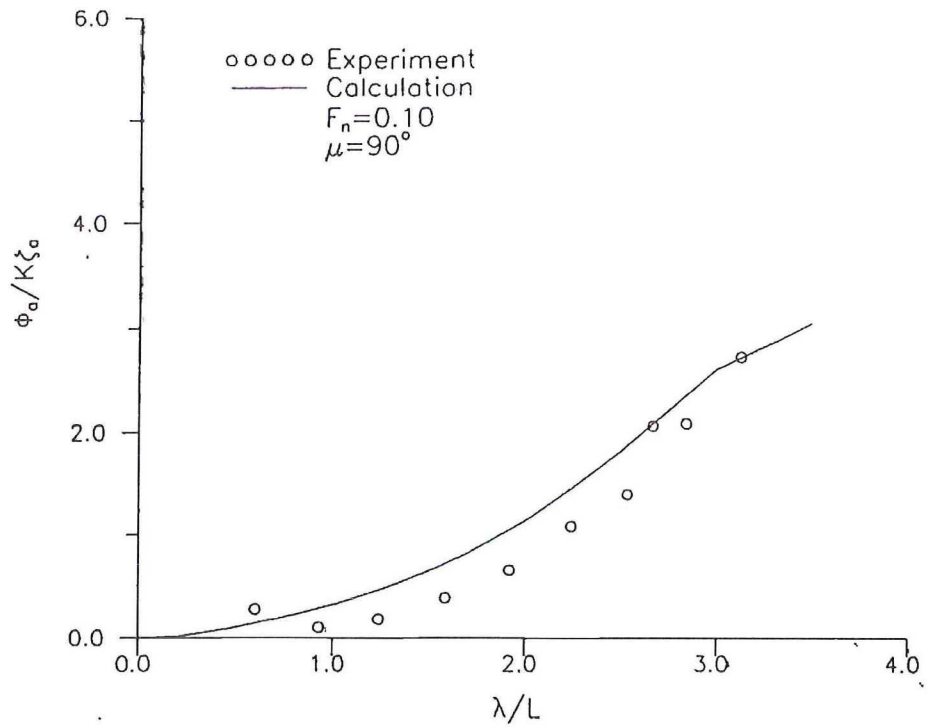


Fig.15 Calculated and measured roll transfer function

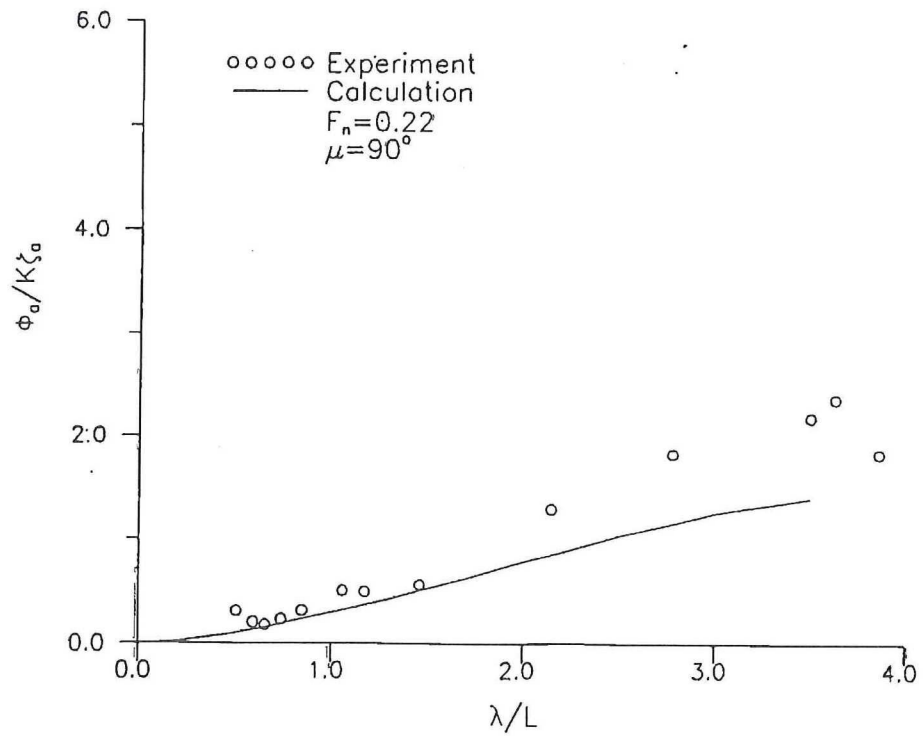


Fig.16 Calculated and measured roll transfer function

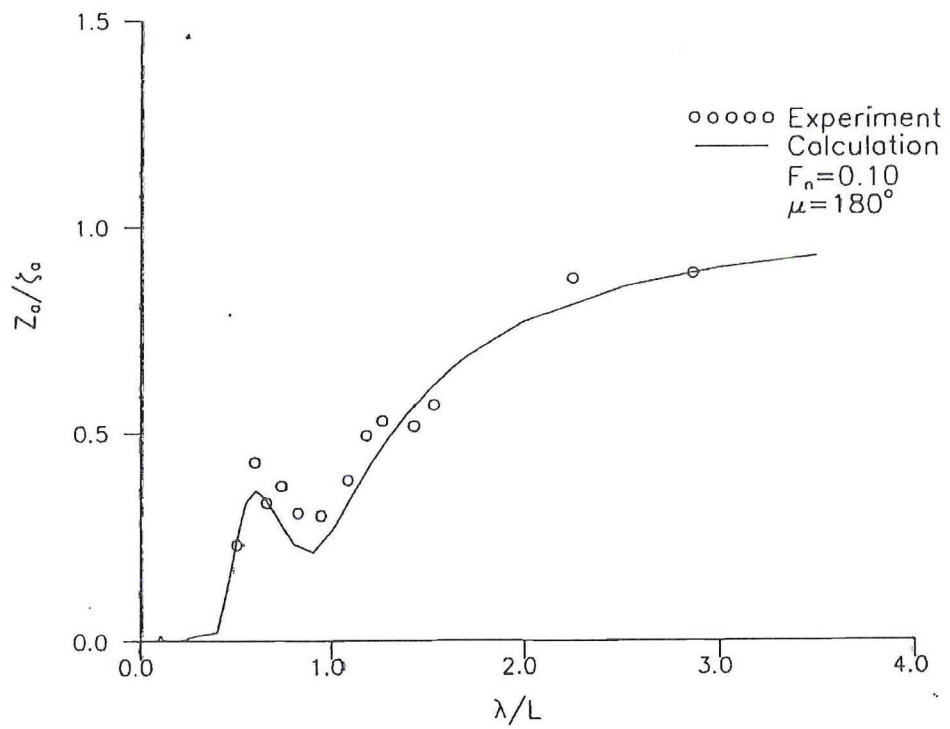


Fig.17 Calculated and measured heave transfer function

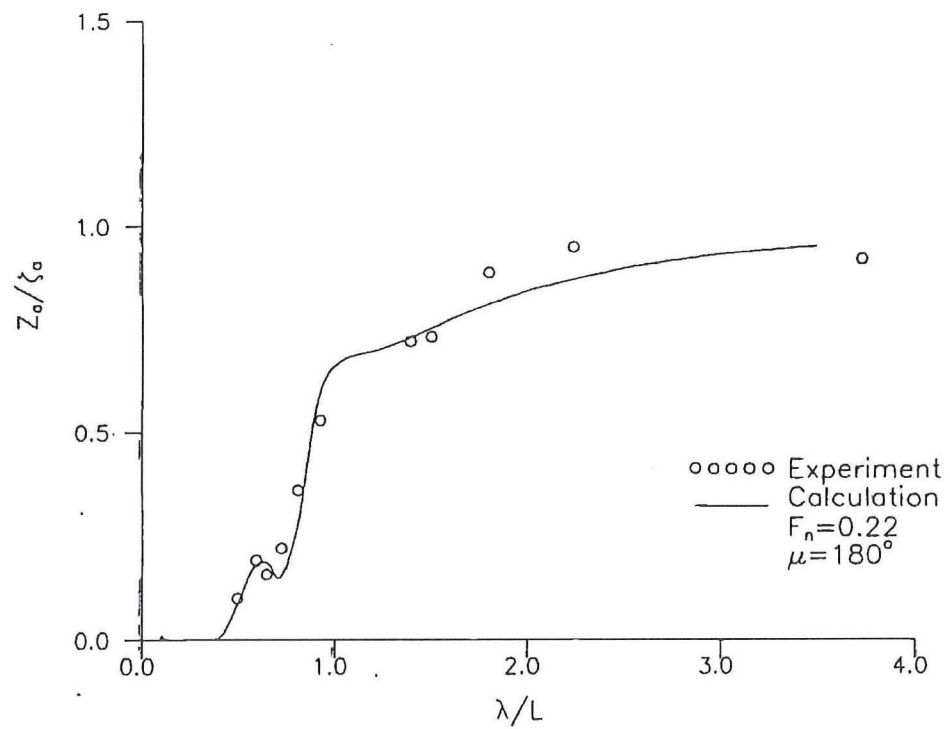


Fig.18 Calculated and measured heave transfer function

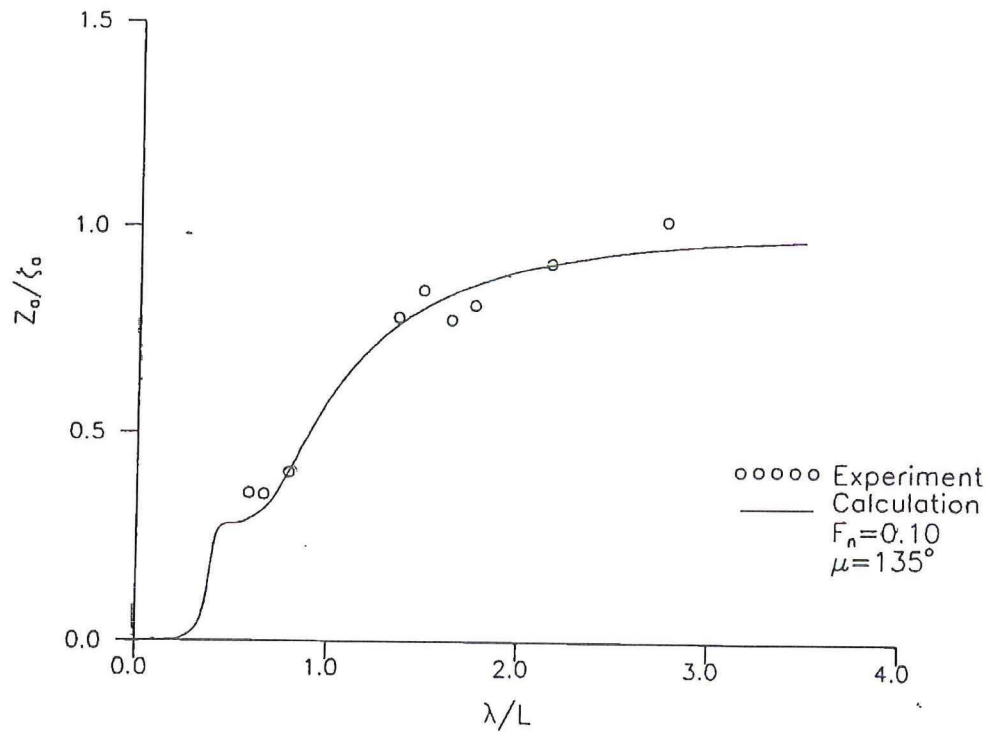


Fig.19 Calculated and measured heave transfer function

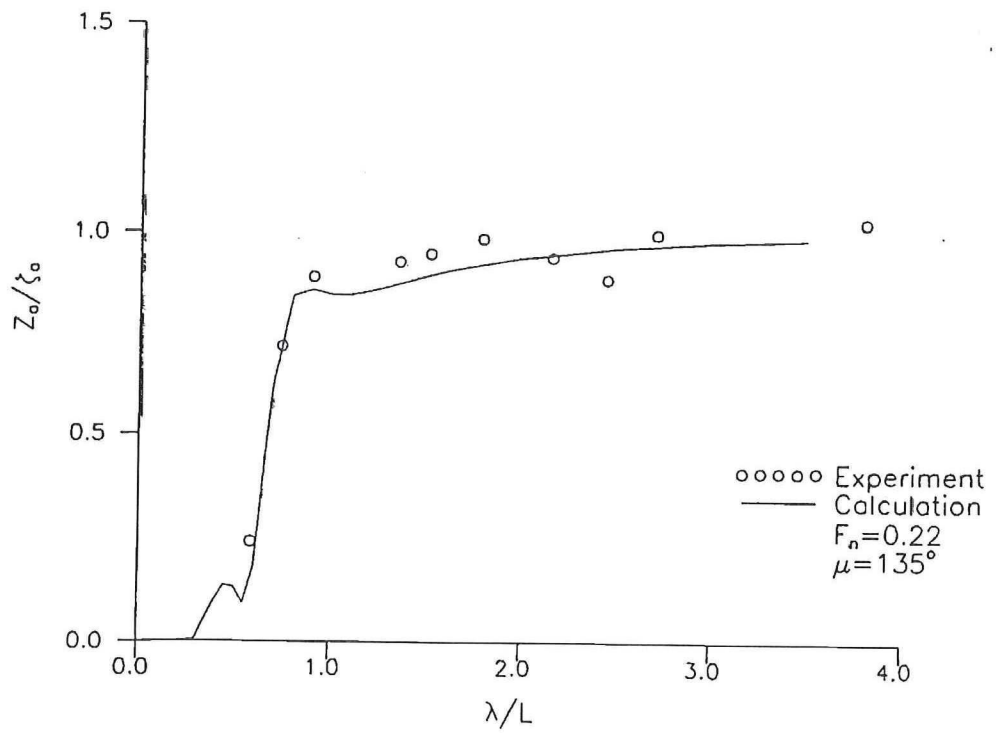


Fig.20 Calculated and measured heave transfer function

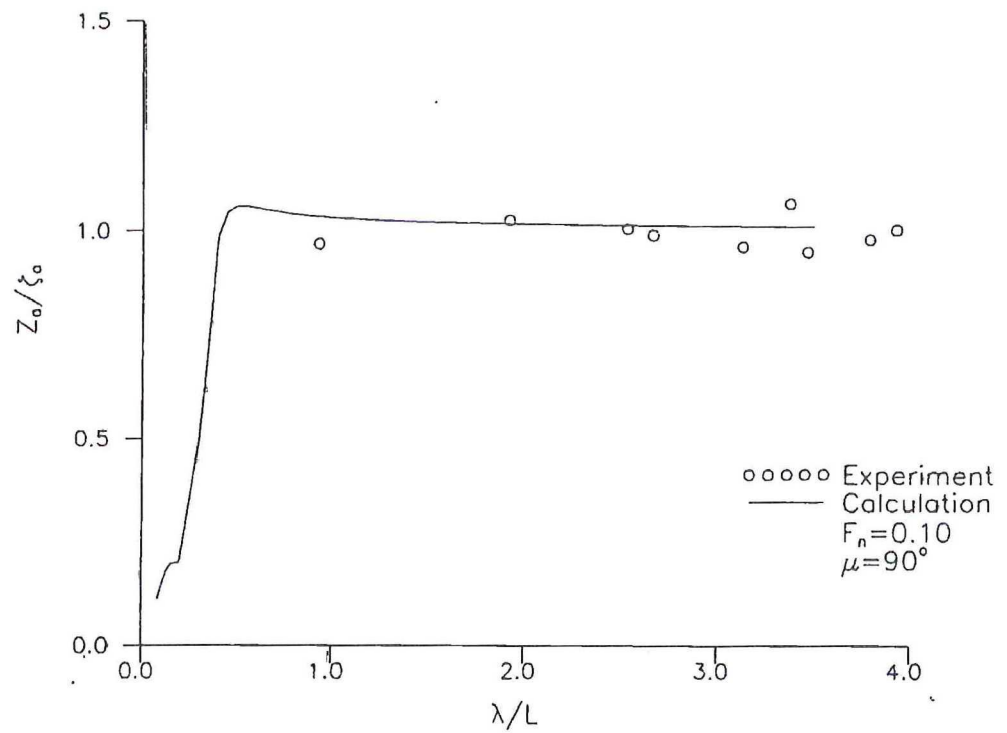


Fig.21 Calculated and measured heave transfer function

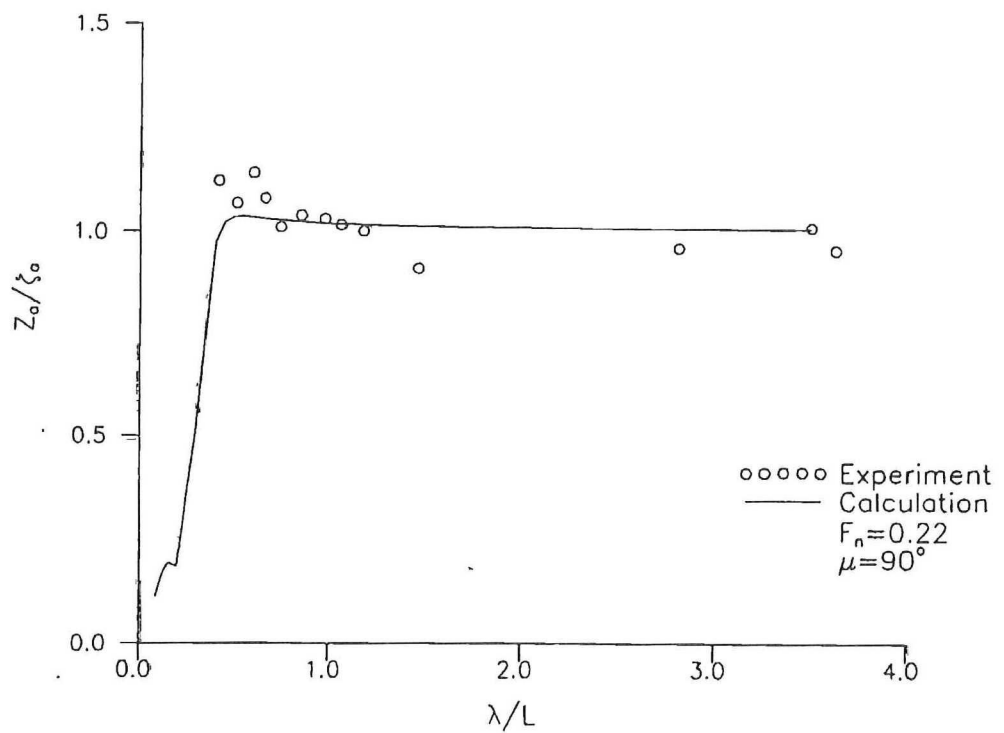


Fig.22 Calculated and measured heave transfer function

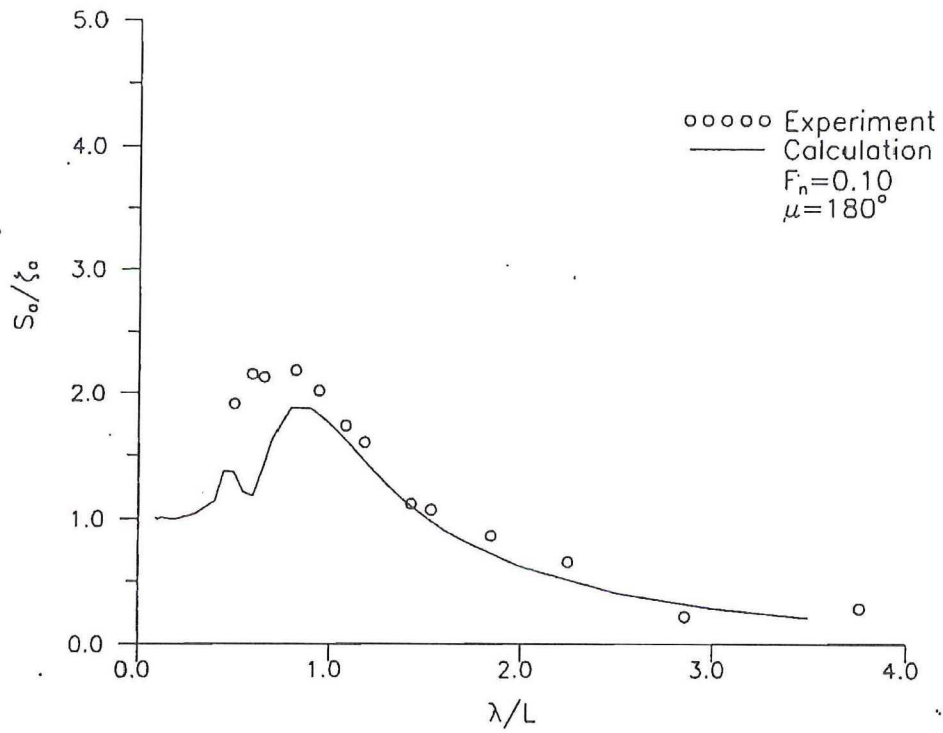


Fig.23 Calculated and measured the relative motion transfer function at station 17

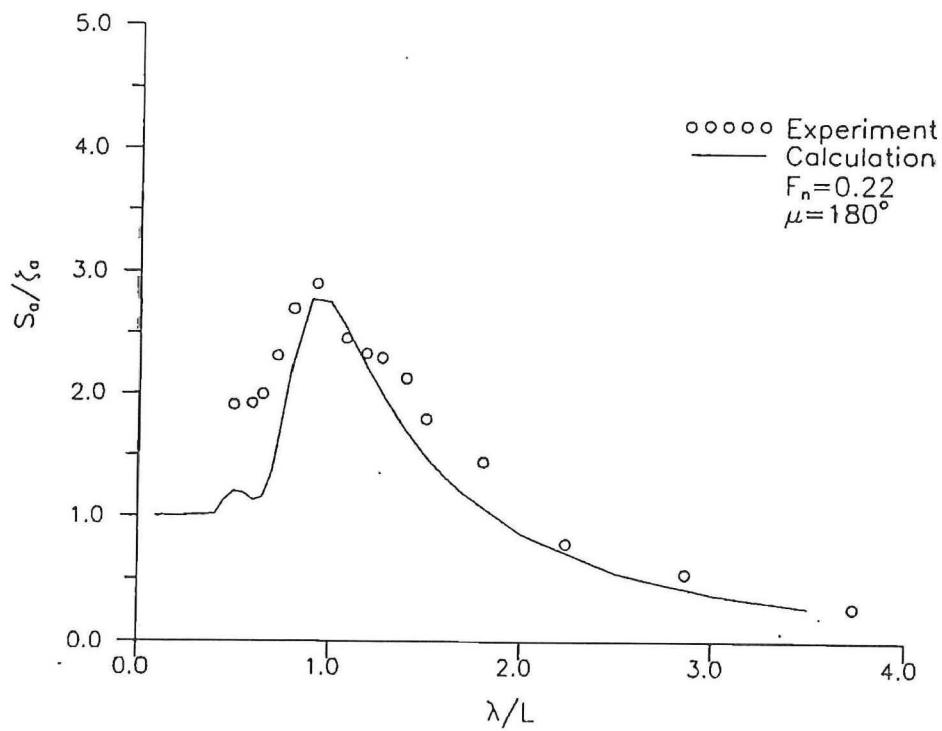


Fig.24 Calculated and measured the relative motion transfer function at station 17

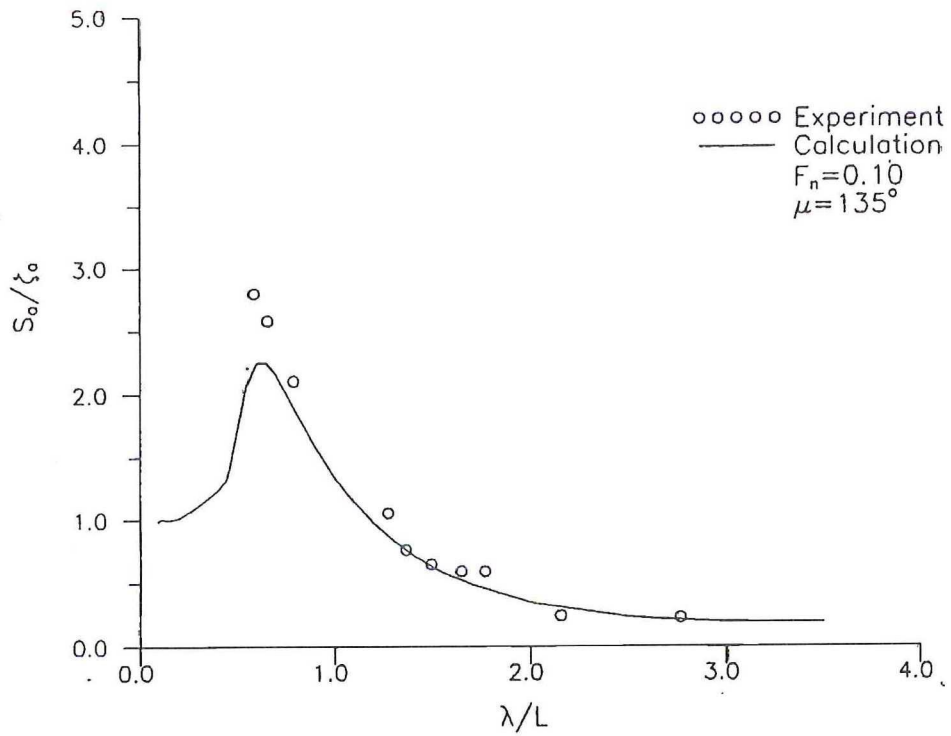


Fig.25 Calculated and measured the relative motion transfer function at station 17

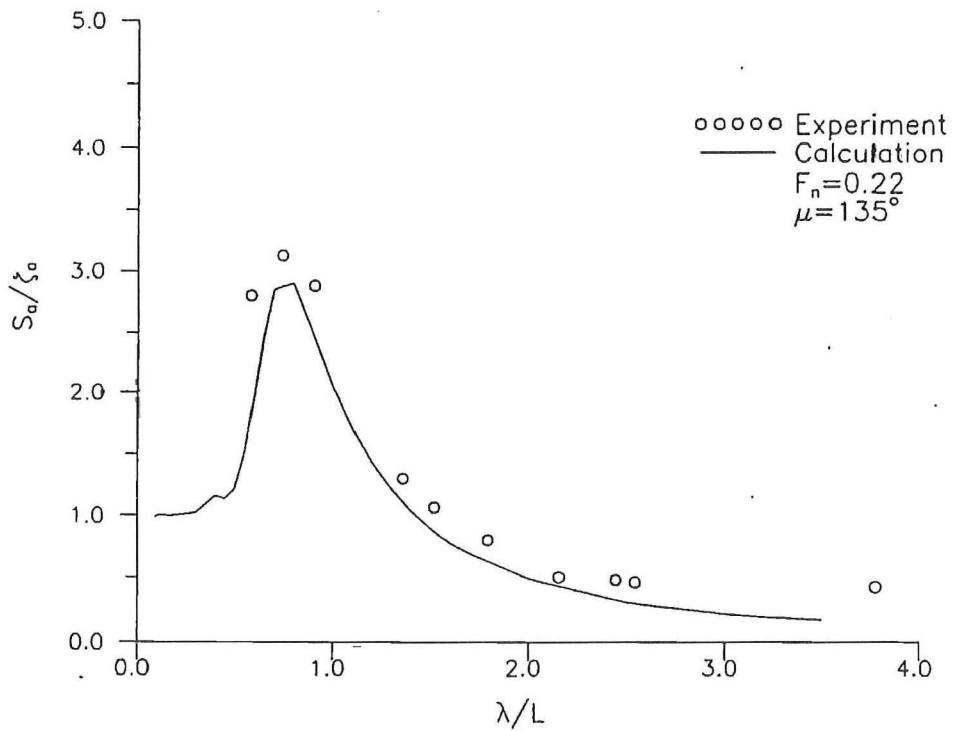


Fig.26 Calculated and measured the relative motion transfer function at station 17

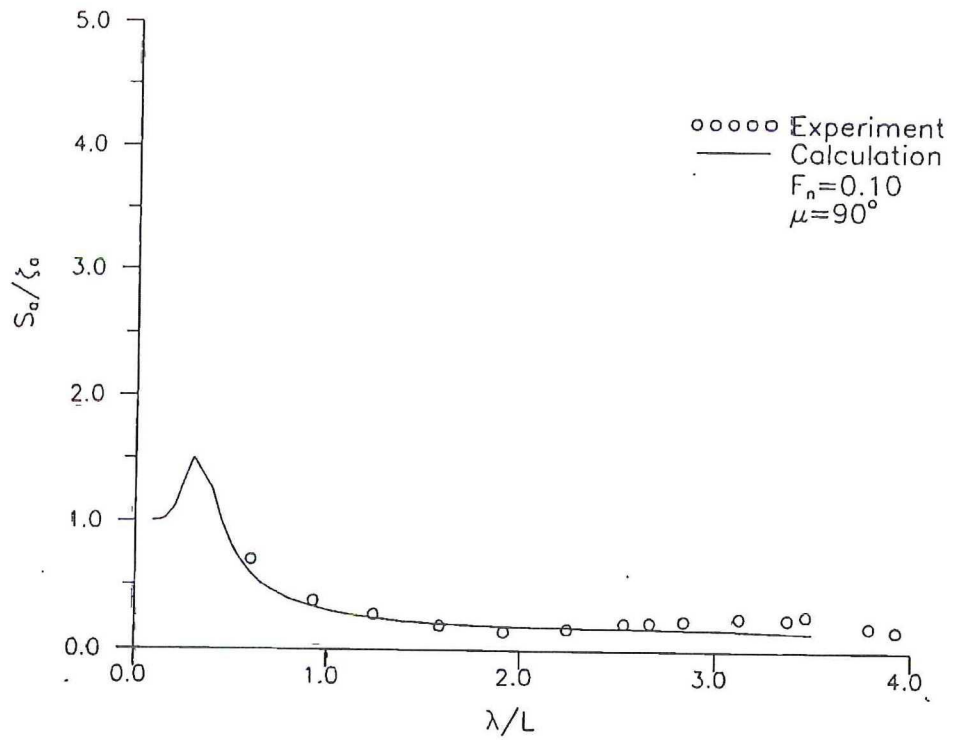


Fig.27 Calculated and measured the relative motion transfer function at station 17

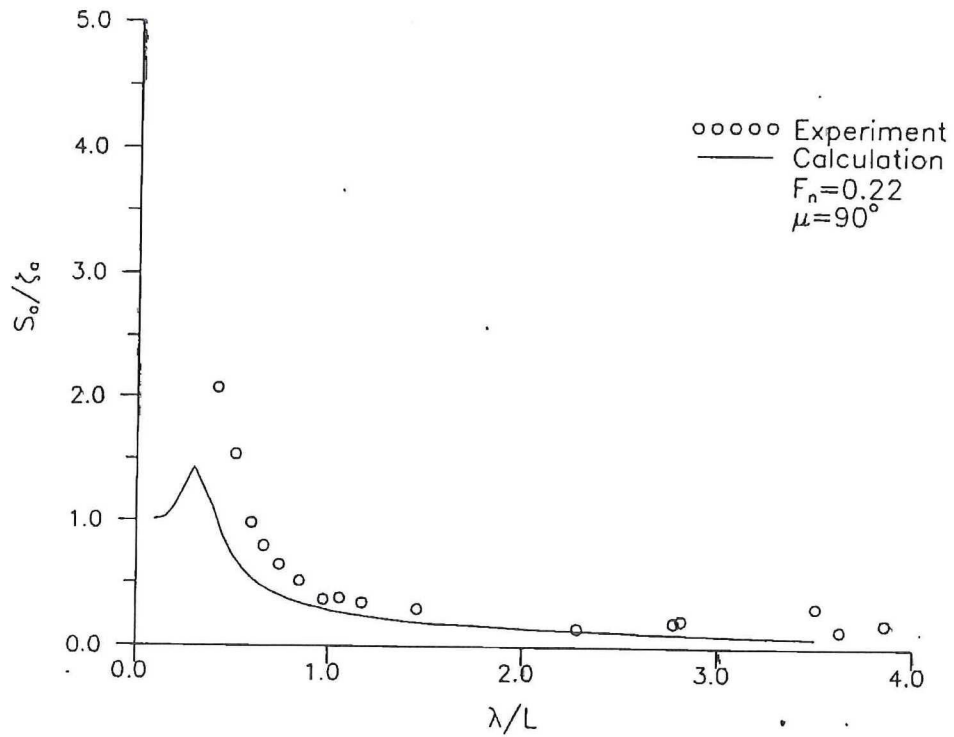


Fig.28 Calculated and measured the relative motion transfer function at station 17

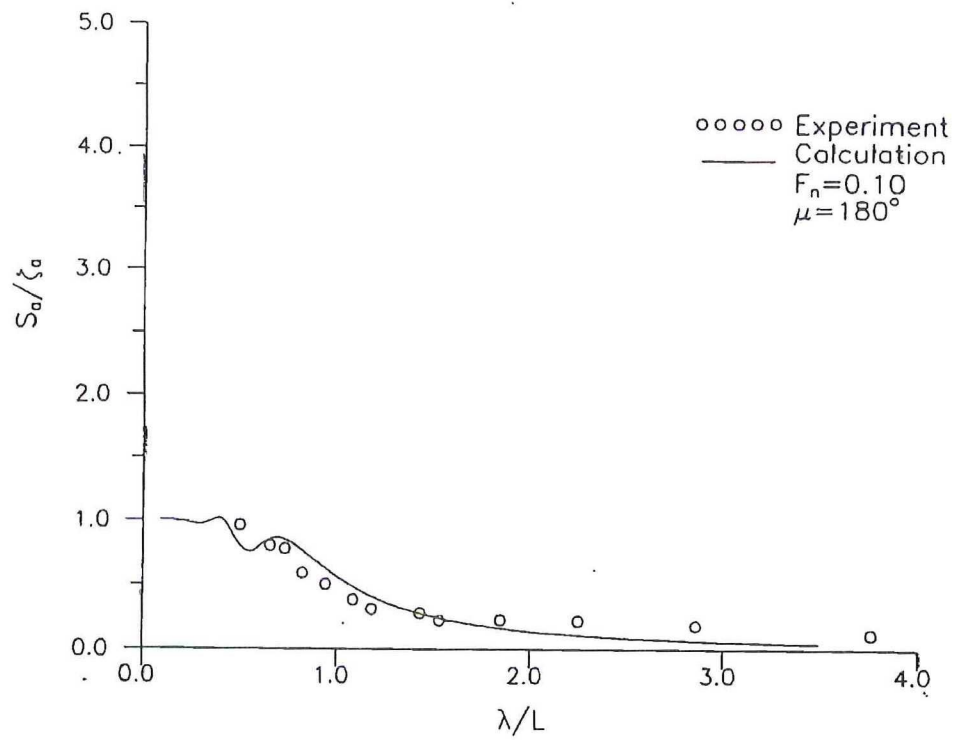


Fig.29 Calculated and measured the relative motion transfer function at station 14

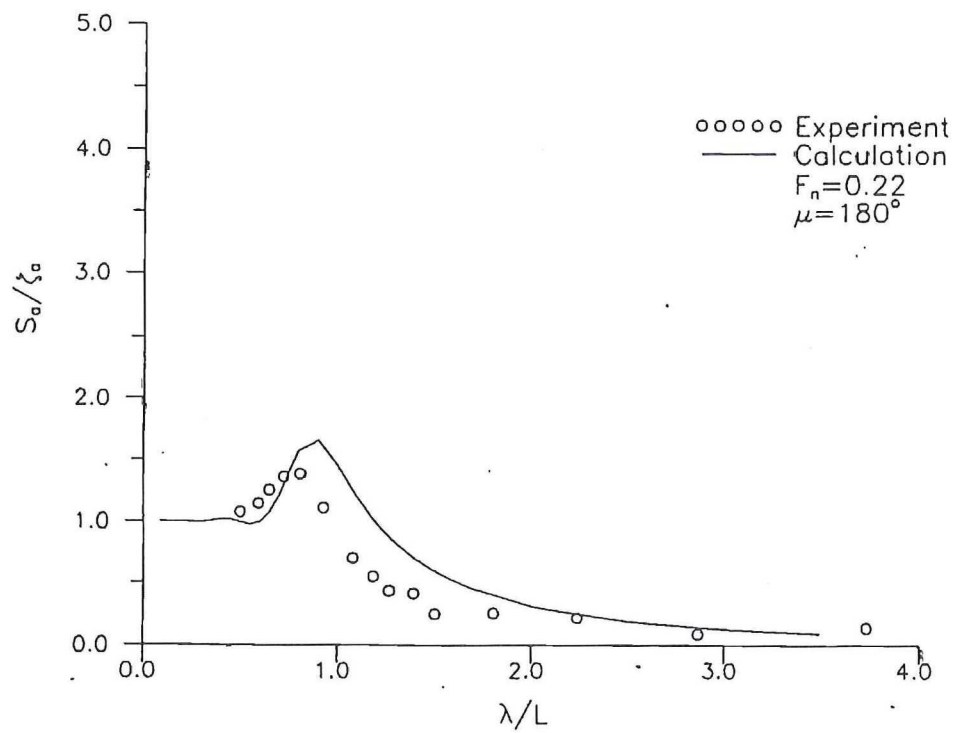


Fig.30 Calculated and measured the relative motion transfer function at station 14

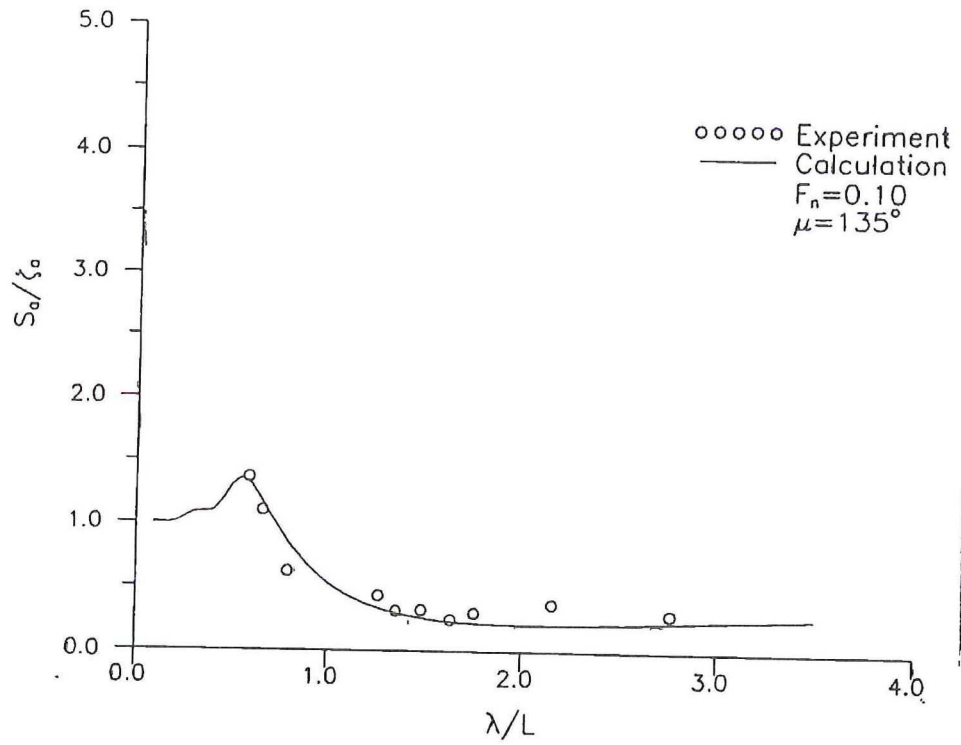


Fig.31 Calculated and measured the relative motion transfer function at station 14

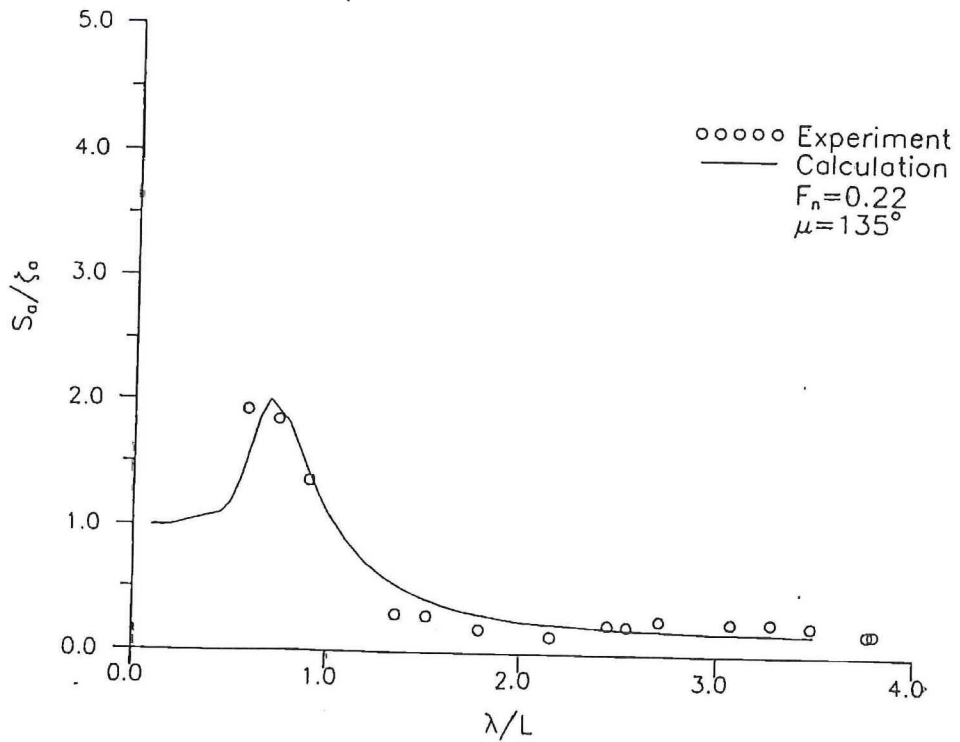


Fig.32 Calculated and measured the relative motion transfer function at station 14

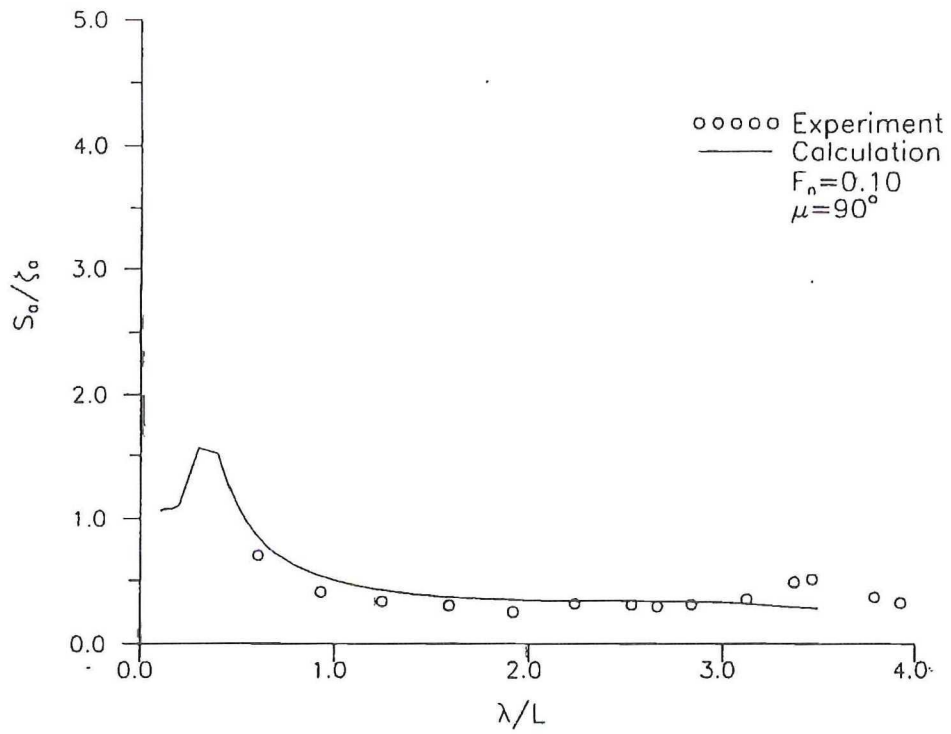


Fig.33 Calculated and measured the relative motion transfer function at station 14

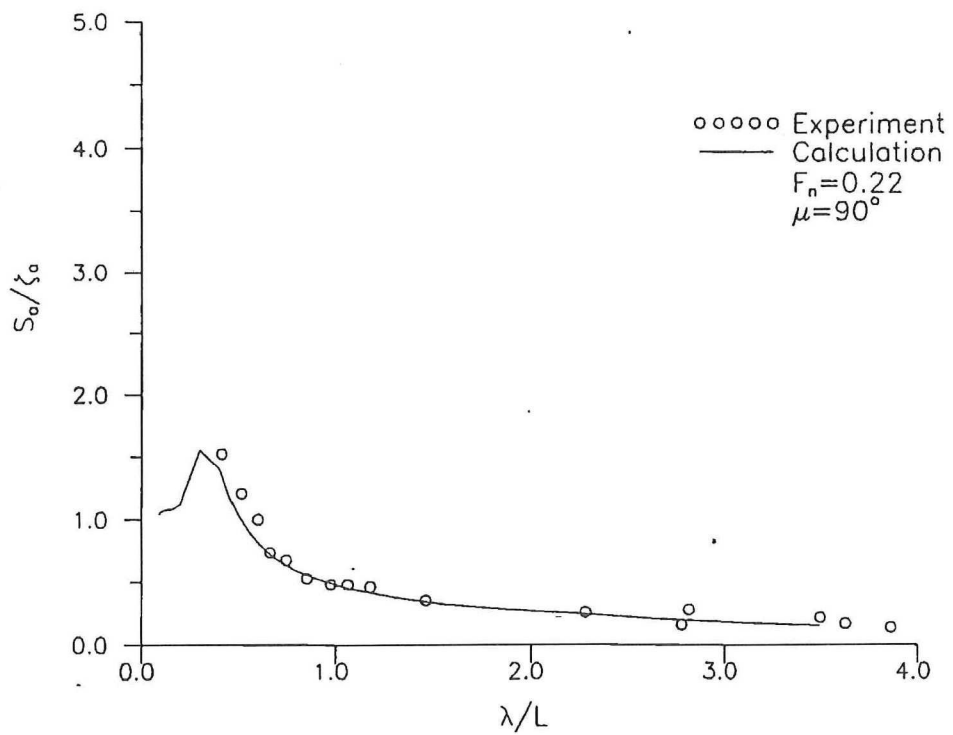


Fig.34 Calculated and measured the relative motion transfer function at station 14

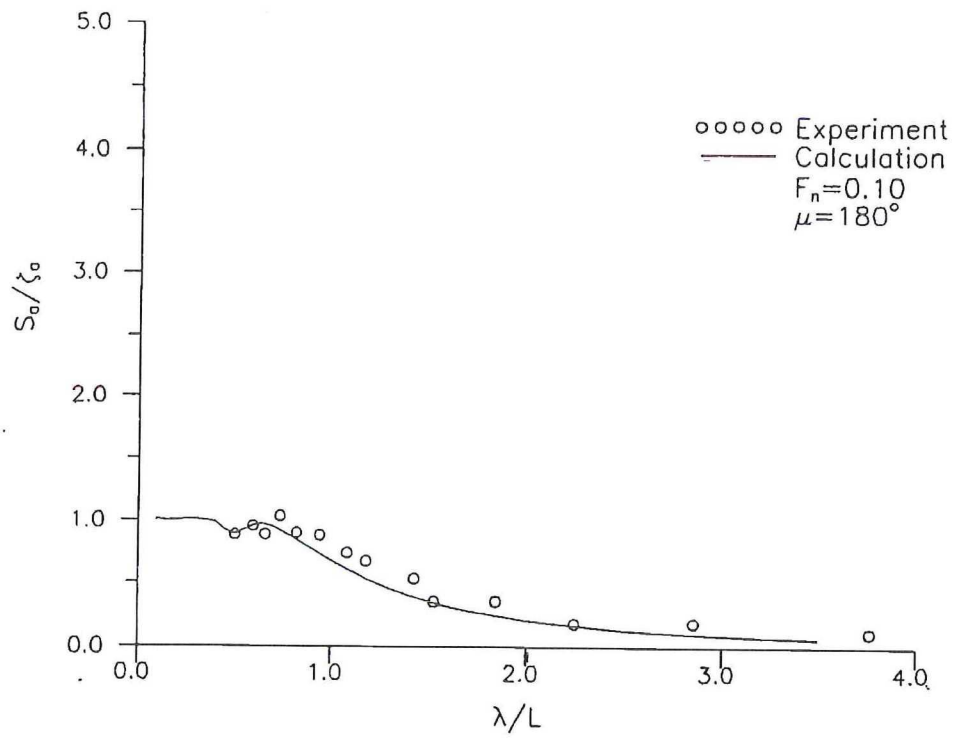


Fig.35 Calculated and measured the relative motion transfer function at station 10

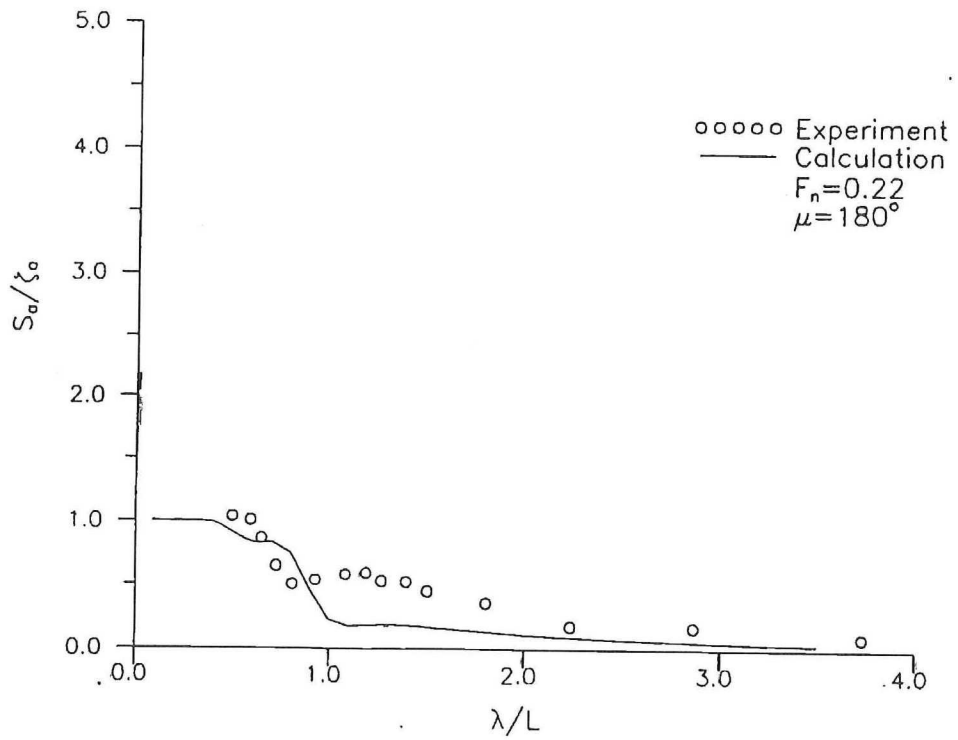


Fig.36 Calculated and measured the relative motion transfer function at station 10

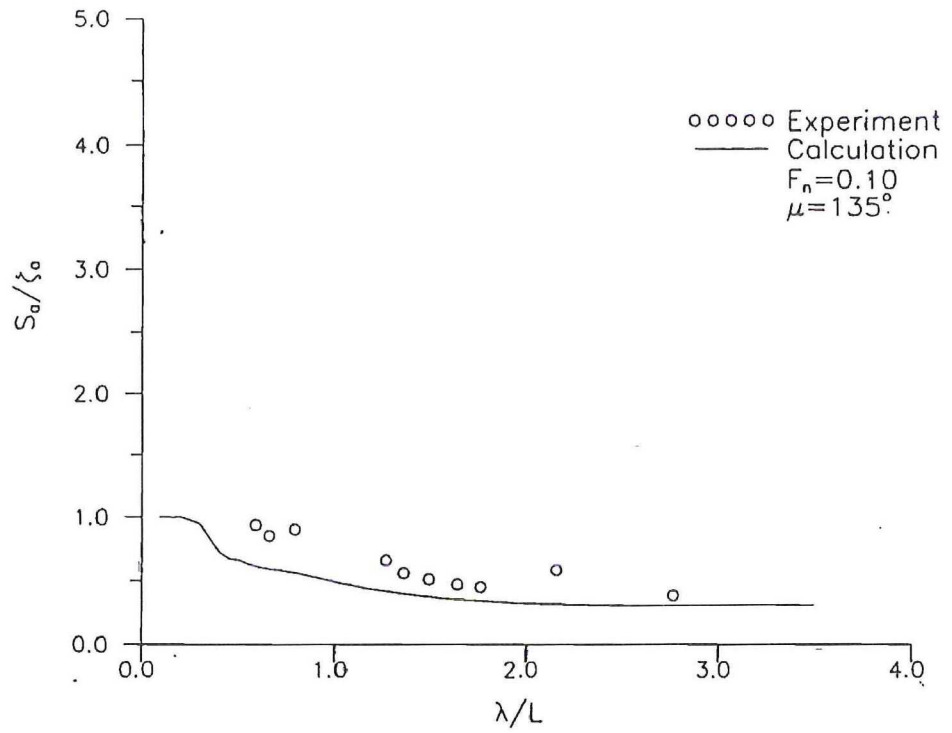


Fig.37 Calculated and measured the relative motion transfer function at station 10

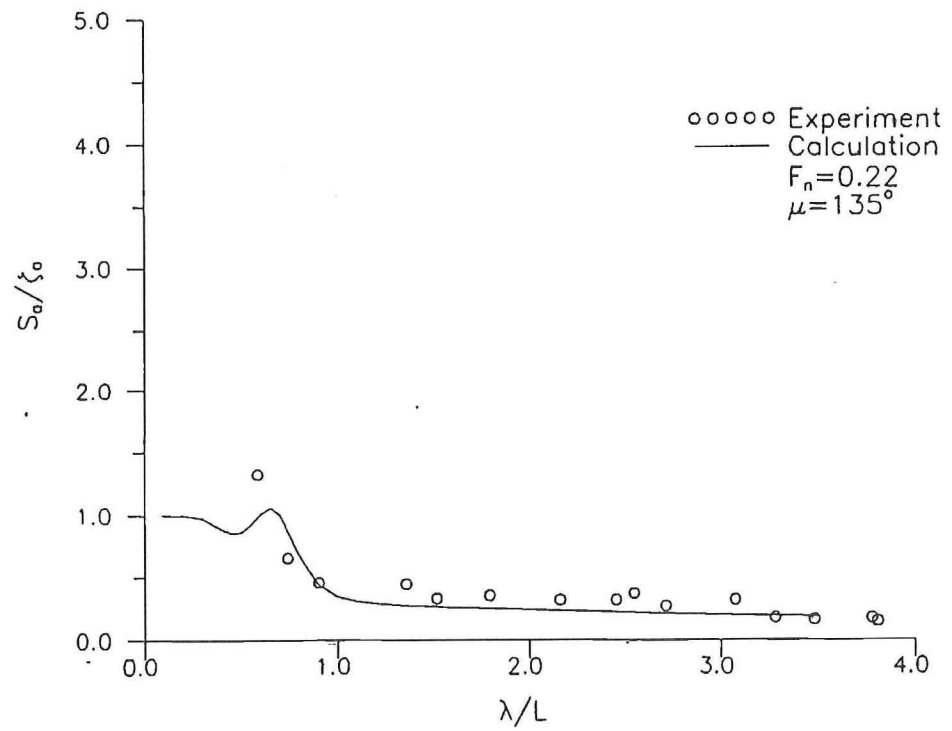


Fig.38 Calculated and measured the relative motion transfer function at station 10

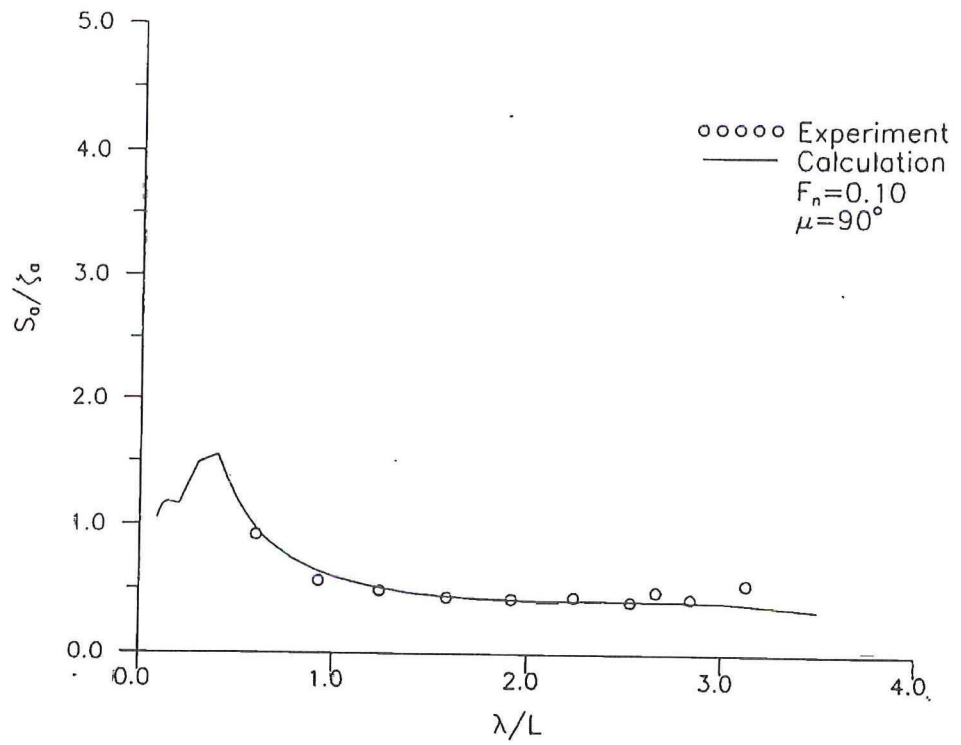


Fig.39 Calculated and measured the relative motion transfer function at station 10

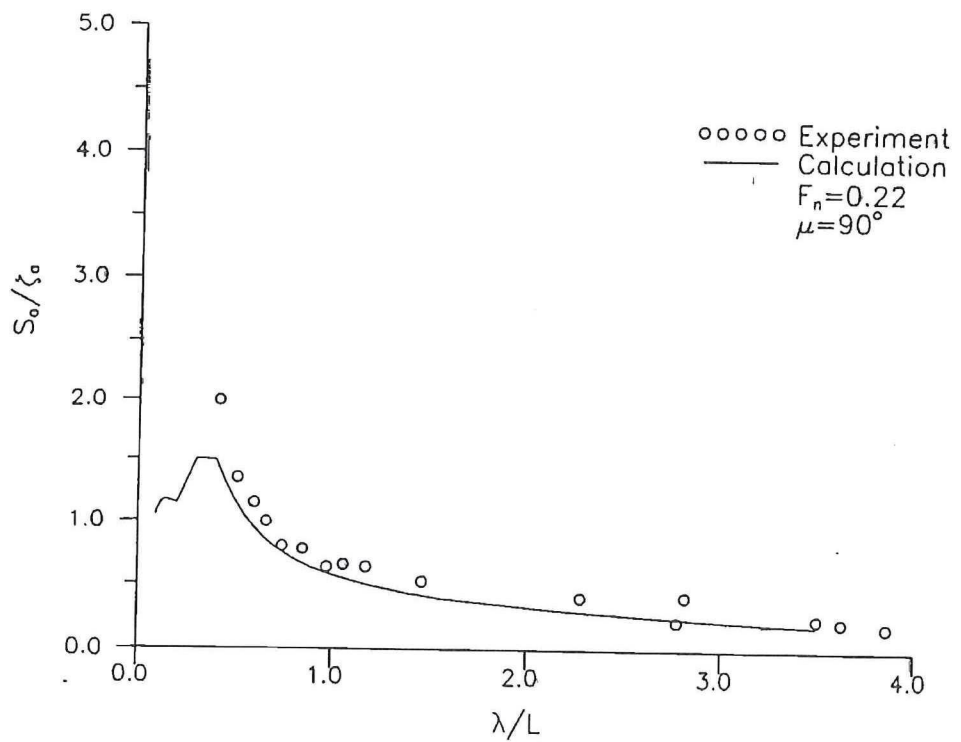


Fig.40 Calculated and measured the relative motion transfer function at station 10

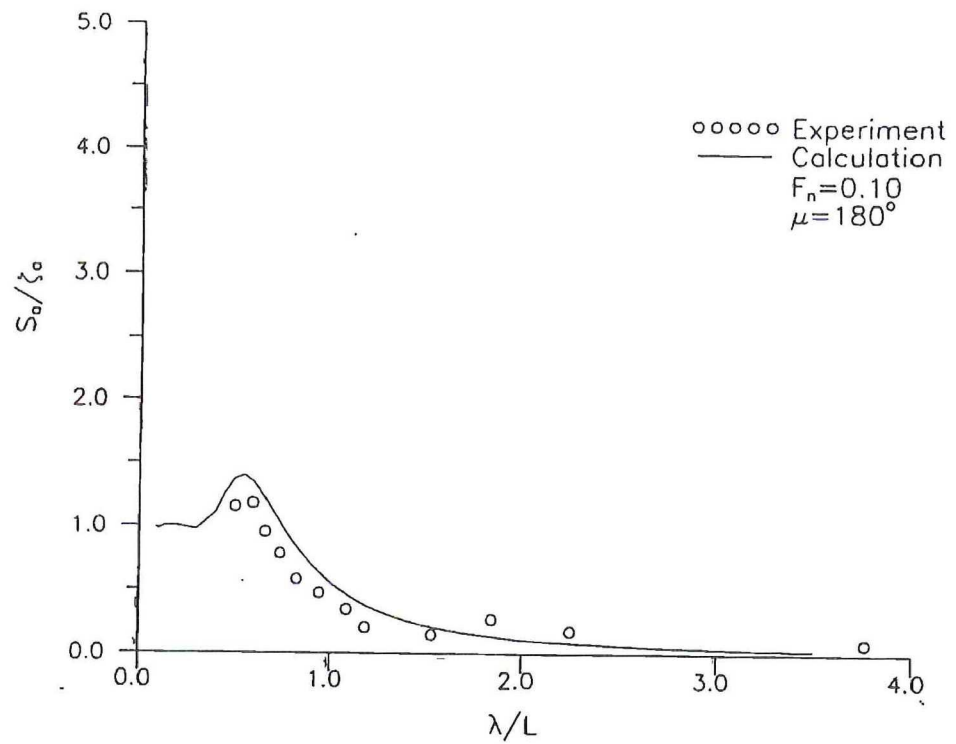


Fig.41 Calculated and measured the relative motion transfer function at station 5

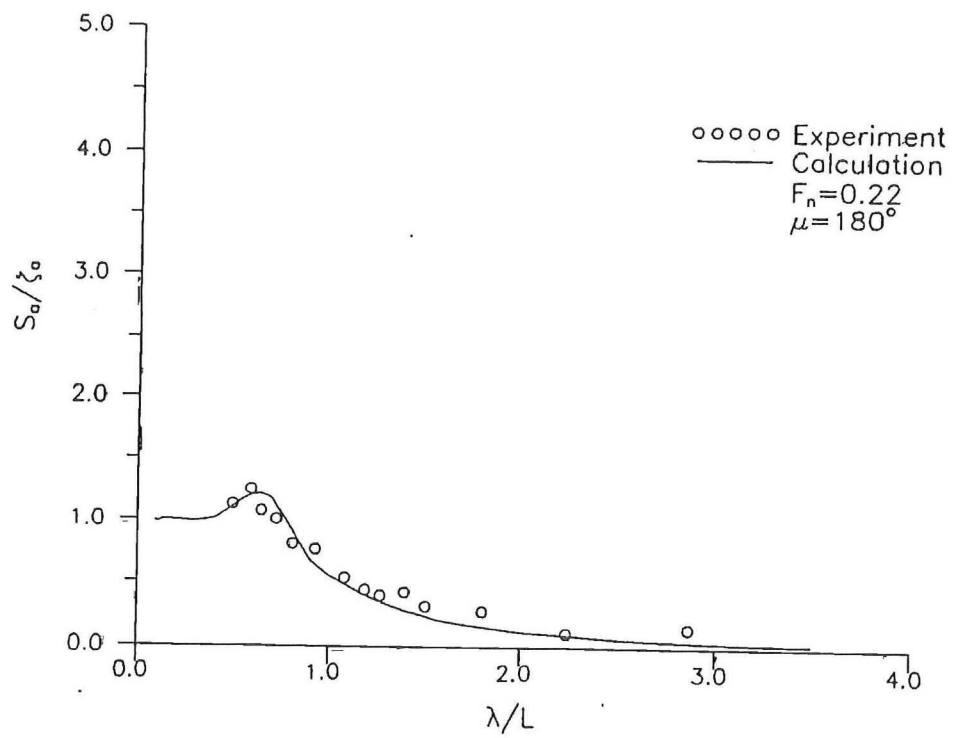


Fig.42 Calculated and measured the relative motion transfer function at station 5

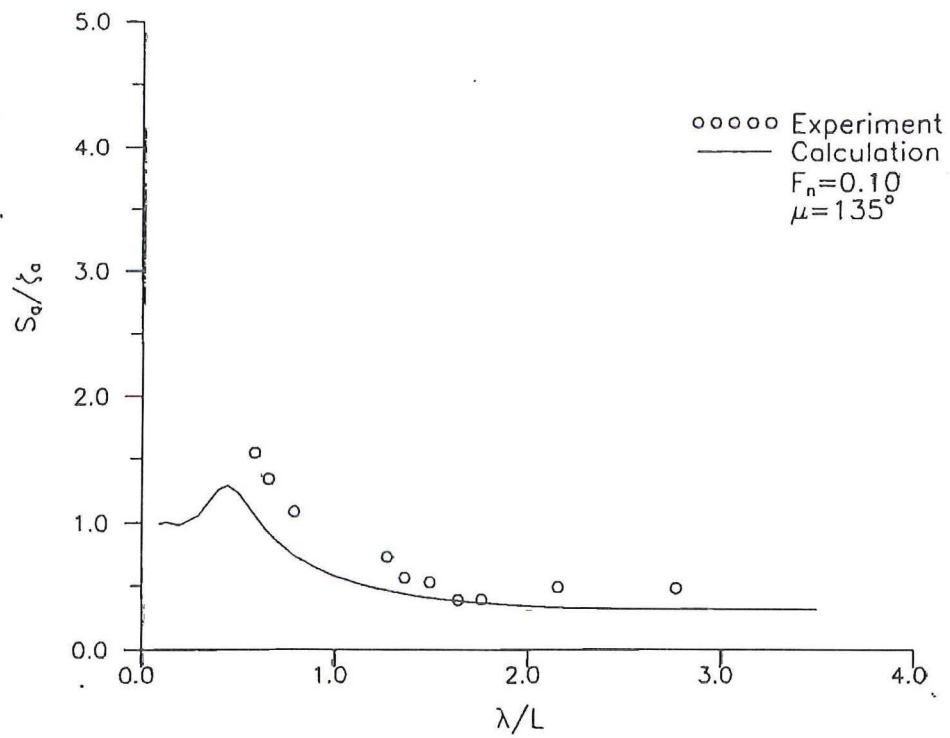


Fig.43 Calculated and measured the relative motion transfer function at station 5

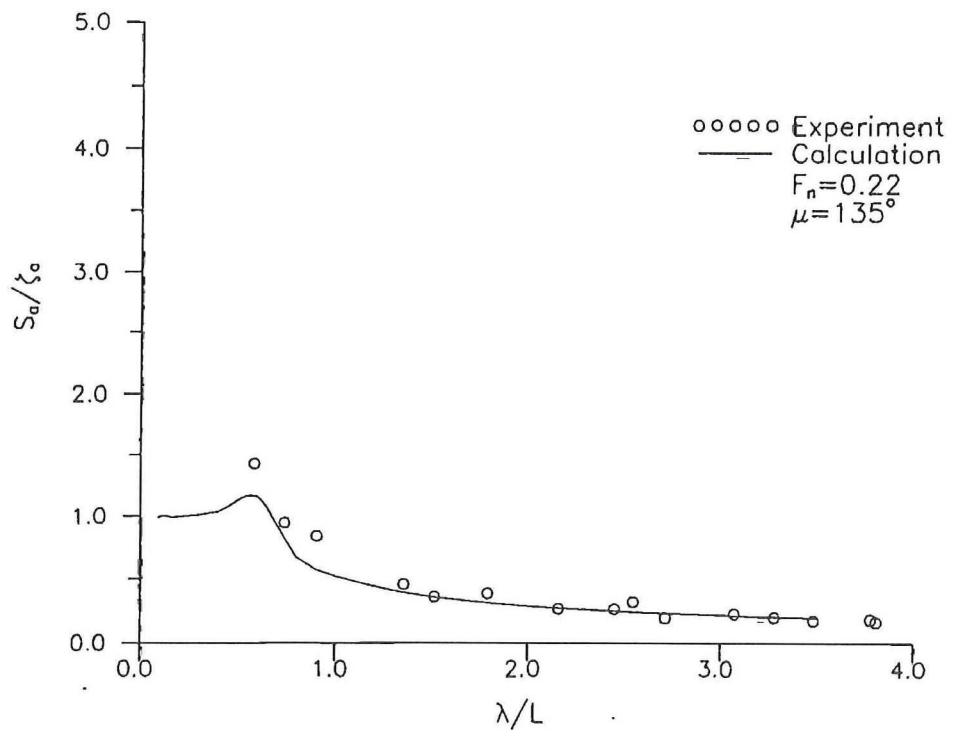


Fig.44 Calculated and measured the relative motion transfer function at station 5

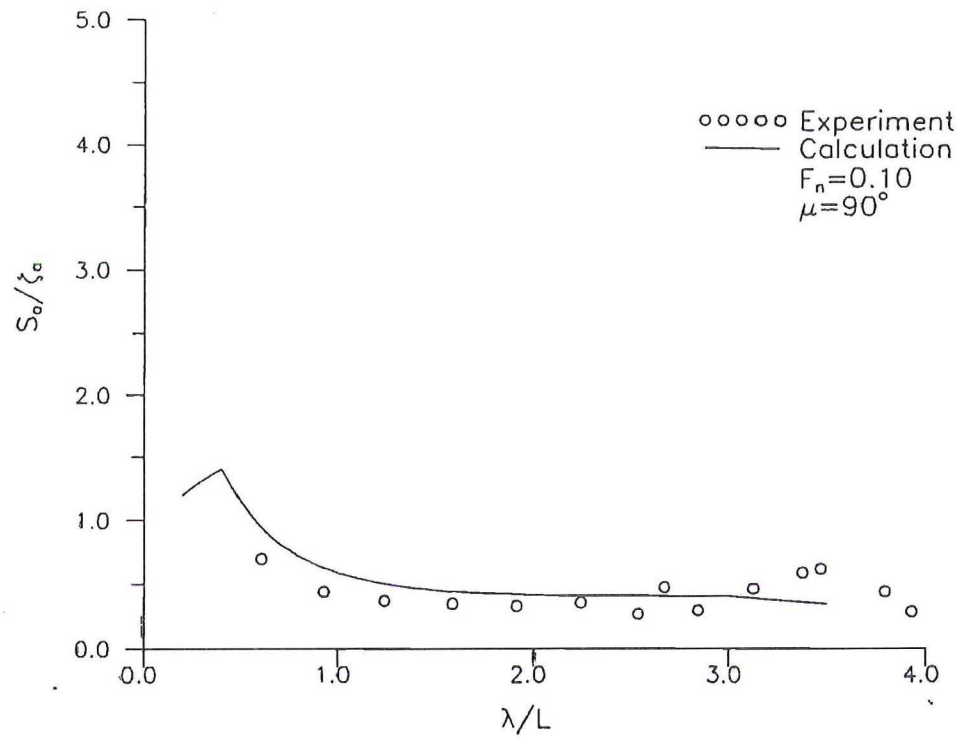


Fig.45 Calculated and measured the relative motion transfer function at station 5

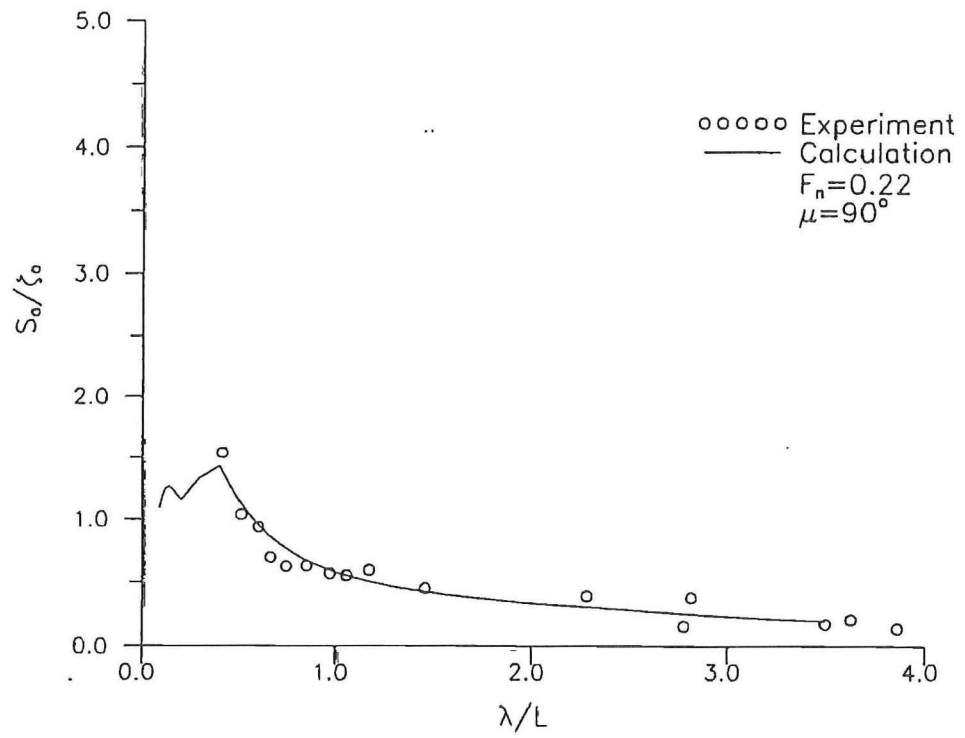


Fig.46 Calculated and measured the relative motion transfer function at station 5

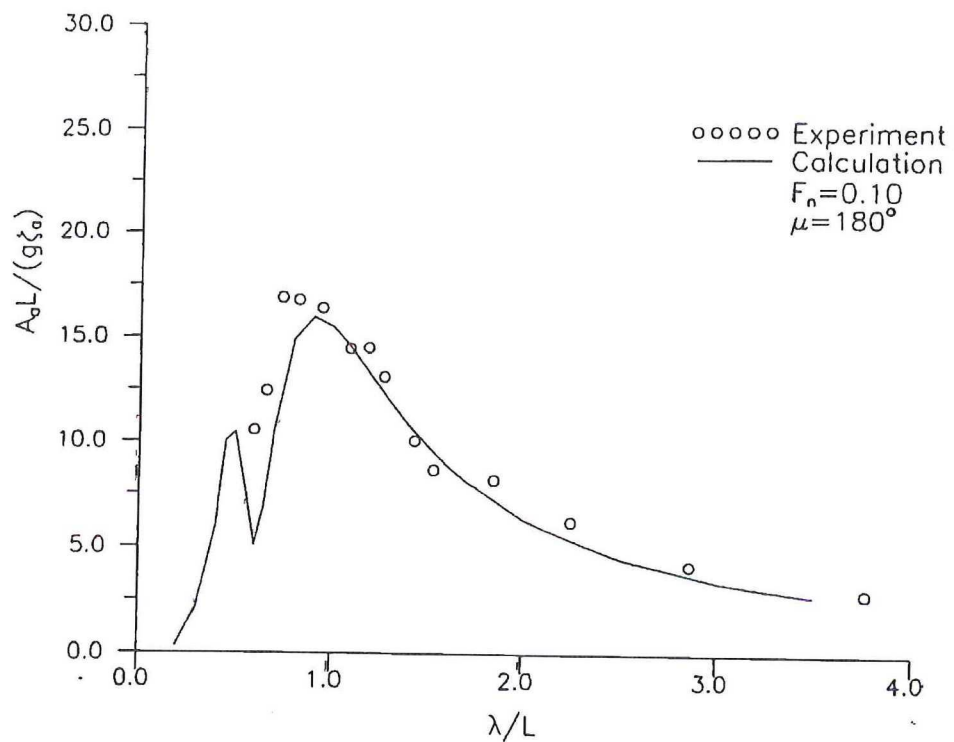


Fig.47 Calculated and measured the vertical acceleration transfer function at station 17

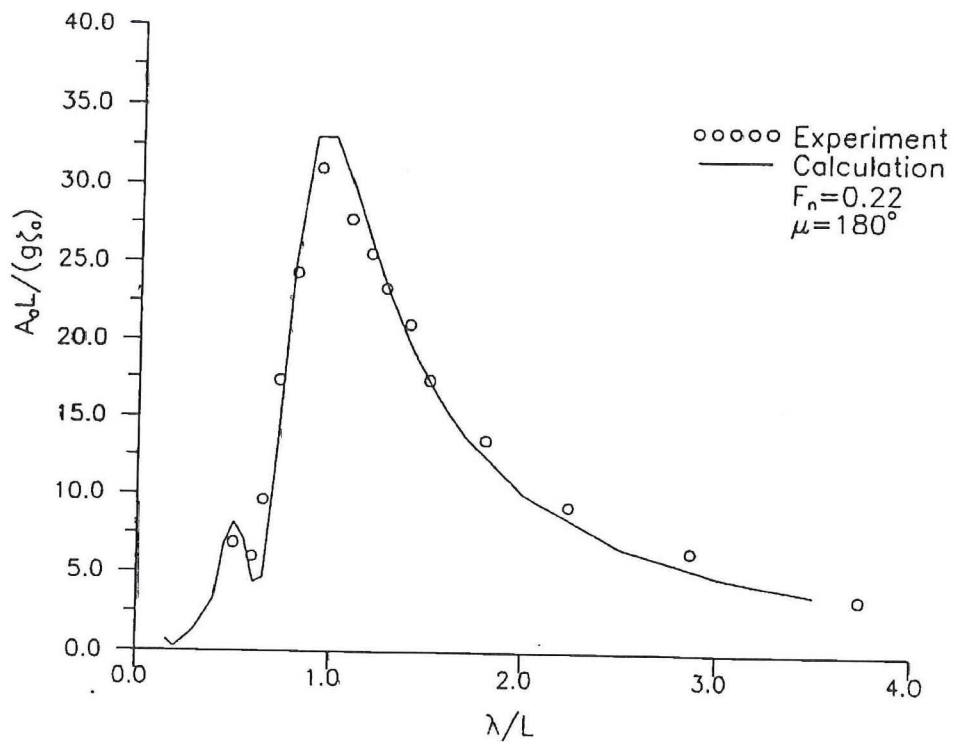


Fig.48 Calculated and measured the vertical acceleration transfer function at station 17

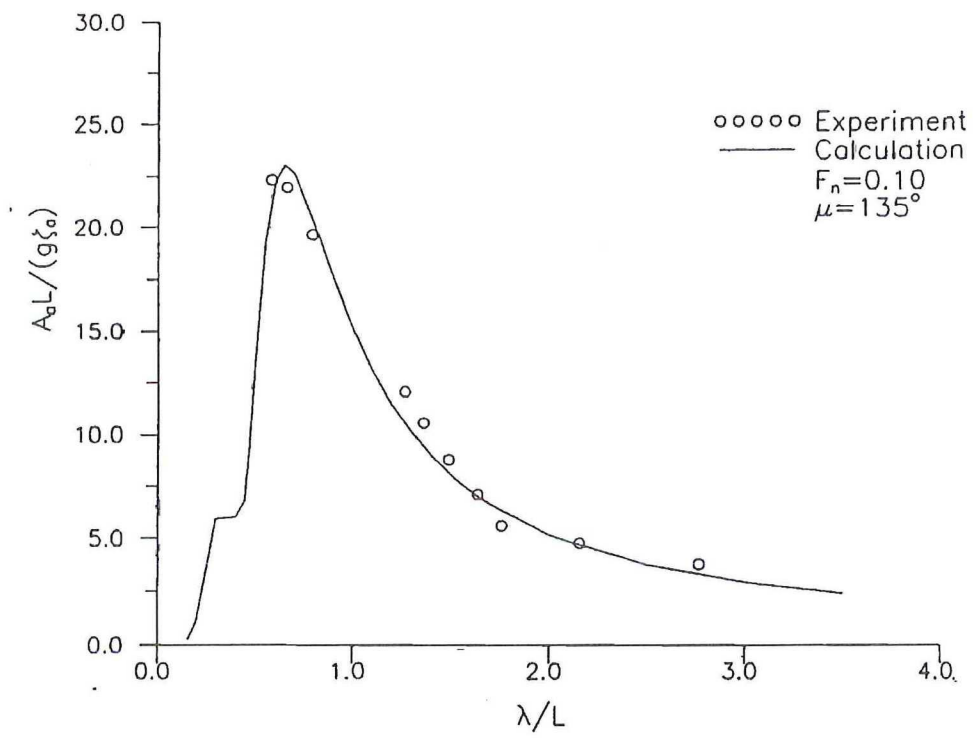


Fig.49 Calculated and measured the vertical acceleration transfer function at station 17

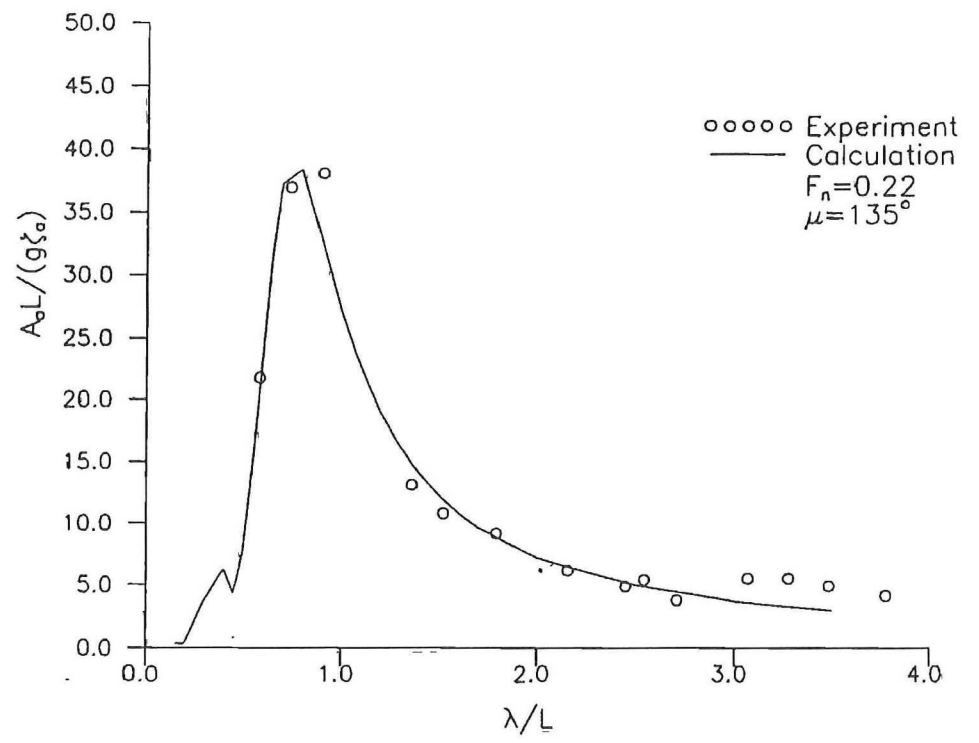


Fig.50 Calculated and measured the vertical acceleration transfer function at station 17

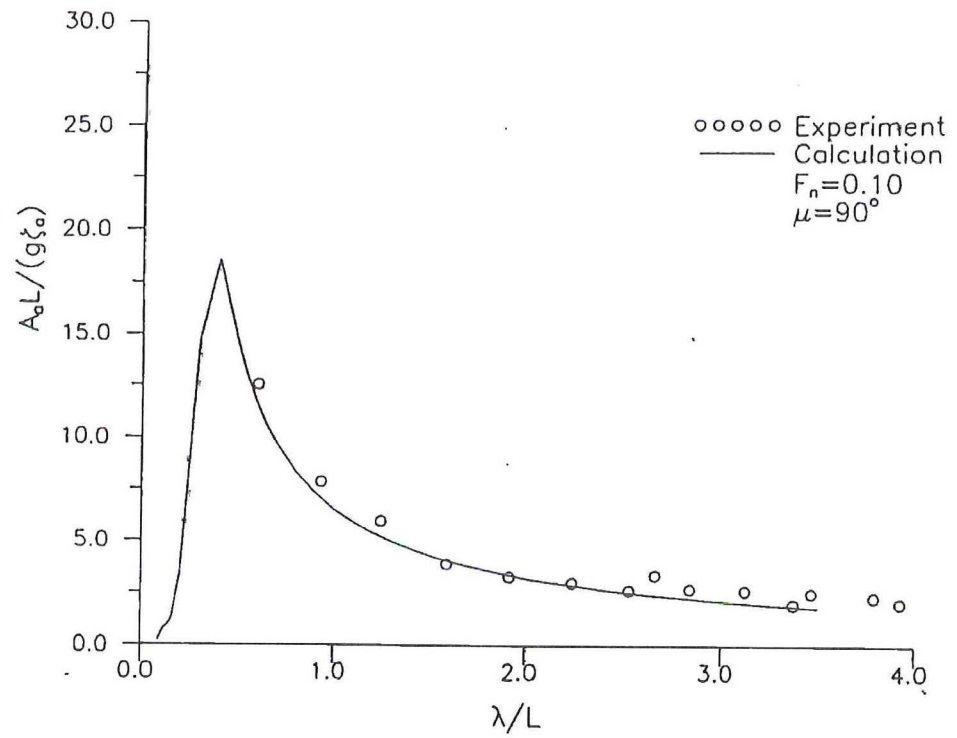


Fig.51 Calculated and measured the vertical acceleration transfer function at station 17

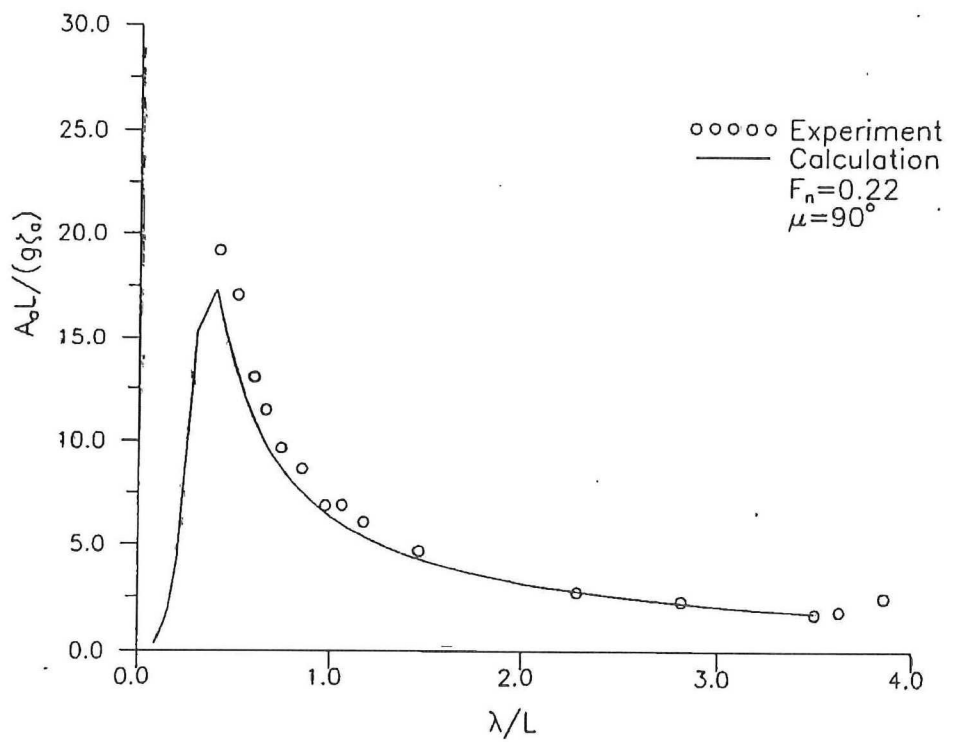


Fig.52 Calculated and measured the vertical acceleration transfer function at station 17

